Available online at www.sciencedirect.com
ScienceDirect
Lithos 91 (2006) 150–172
LITHOS
www.elsevier.com/locate/lithos

Primary magmas at Oldoinyo Lengai: The role of olivine melilitites

Jörg Keller [a,*], Anatoly N. Zaitsev [a,b,c], Daniel Wiedenmann [a]

[a] Institut für Mineralogie, Petrologie und Geochemie, Universität Freiburg, Albertstrasse 23b, 79104 Freiburg, Germany
[b] Department of Mineralogy, St. Petersburg State University, St. Petersburg 199034, Russia
[c] Department of Mineralogy, The Natural History Museum, Cromwell Road, London SW7 5BD, UK

Received 1 August 2005; accepted 13 March 2006
Available online 13 June 2006

Abstract

The paper describes olivine melilitites at Oldoinyo Lengai, Tanzania, and from tuff cones from the Tanzanian rift valley in the vicinity of Oldoinyo Lengai. Oldoinyo Lengai is the only active carbonatite volcano and is distinguished by its alkali-rich natrocarbonatites. Lengai is also unique for its extreme peralkaline silicate lavas related directly to the natrocarbonatites. Primitive olivine melilitites are, according to their Mg# and Ni, Cr contents, the only candidates in the Lengai area for primary melt compositions. Incompatible trace elements, including REE, constrain the melting process in their sub-lithospheric sources to very low degrees of partial melting in the garnet stability field. The strong peralkaline trend at Oldoinyo Lengai is already recognisable in these primary or near-primary melts. More evolved olivine melilitites, with Mg# <60 allow the fractionation line in its major and trace element expressions to be followed. Nevertheless, a large compositional gap separates the olivine melilitites and olivine-poorer melilitites from the phonolites and nephelinites that form the bulk of the Lengai cone. These silicate lavas show a high degree of peralkalinity and are highly evolved with very low Mg, Ni and Cr. Prominent examples of the recent evolution are the combeite–wollastonite nephelinites that are unique for Lengai. In their Sr, Nd, and Pb isotope relationships the olivine melilitites define a distinct group with the most depleted Sr and Nd ratios and the most radiogenic Pb isotopes. They are closest to a supposed HIMU end member of the Lengai evolution, which is characterised by an extreme spread in isotopic ratios, explained as a mixing line between HIMU and EM1-like mantle components.

Keywords: Oldoinyo Lengai; Carbonatite volcano; Olivine melilitites; Primary magmas; Magmatic evolution; Sr–Nd–Pb isotopes; Peralkalinity

1. Introduction

Oldoinyo Lengai is the only active carbonatite volcano in the world and is known for the unusually alkali-rich composition of its carbonatite lavas. Natrocarbonatite characterises the recent activity which is expressed by the current quiet effusions in the northern summit crater. It is inferred from historical reports that this type of activity goes back more than 100 years (Dawson et al., 1995a). A natrocarbonatite lava platform, similar to the recent crater filling, was present when the first explorers reached the summit in 1904 (Uhlig, 1907). Explosive eruptions have interrupted the quiet extrusion of natrocarbonatite several times in the historical record, ejecting mixed ashes and lapilli of a silicate melt that is contemporaneously available at Oldoinyo Lengai with the natrocarbonatite (Dawson et al., 1968; Keller and Krafft, 1990; Dawson et al., 1992). More than 95 vol.% of the volcano is composed of silicate lavas and pyroclastics (Dawson, 1962, 1989).

* Corresponding author. Tel.: +49 761 2036404; fax: +49 761 2036407.
E-mail address: Joerg.Keller@minpet.uni-freiburg.de (J. Keller).

0024-4937/$ - see front matter © 2006 Elsevier B.V. All rights reserved.
doi:10.1016/j.lithos.2006.03.014

An eruption in 1993 produced natrocarbonatite flows with silicate globules suggested to be testimony of immiscibility phenomena (Church and Jones, 1995; Dawson et al., 1996; Simonetti et al., 1997). The whole evolution of Oldoinyo Lengai is considered geologically young, i.e. belonging entirely to the Quaternary, most likely to the upper Quaternary (McIntyre et al., 1974; Hay, 1989; Dawson et al., 1995a).

2. Silicate lavas of Oldoinyo Lengai—the question of primary compositions

Silicate lavas at Oldoinyo Lengai are dominantly nephelinites and phonolites (Donaldson et al., 1987; Dawson, 1989). These lavas are highly alkaline and reach high levels of peralkalinity ($(Na+K)/Al>1$), which finds its expression in the unusual mineralogy with combeite (ideal formula $Ca_2Na_2(Si_3O_9)$) in the most recent combeite–wollastonite nephelinites (CWN) (Peterson, 1989a; Dawson et al., 1989; Keller and Krafft, 1990; Klaudius and Keller, 2006-this issue). An important feature of all silicate lava samples from Oldoinyo Lengai is their evolved composition. Maximum MgO contents of all published and available analyses (Donaldson et al., 1987; Dawson, 1989; Peterson, 1989a; Keller and Spettel, 1995; Dawson, 1998; Klaudius and Keller, 2006-this issue) do not exceed about 2 wt.% MgO and all Mg# ($100\ Mg/(Mg+Fe^{2+})$), calculated with $Fe_2O_3/FeO=0.15$, are below 30. This raises the question of primary magmas at Oldoinyo Lengai. The highly fractionated nature is underlined by Ni and Cr contents that are consistently ≤ 10 ppm, and the generally enriched incompatible element patterns.

Phonolites extruded from the South crater and dominate in the activity of the primordial cone (Lengai I), while nephelinites characterise the lavas from the northern crater, Lengai II. Lengai II, the combeite–wollastonite nephelinite and natrocarbonatite volcano developed after failure and collapse of the cone of Lengai I (Klaudius and Keller, 2006-this issue).

Mainly based on the isotopic composition, Bell and Dawson (1995), Bell and Simonetti (1996) and Dawson (1998) were able to distinguish two groups of nephelinites, Group I and Group II, respectively. The CWN group forms the lavas of the northern crater and cone, termed Lengai II. A liquid immiscibility relationship between these peralkaline, evolved and carbonated CWN compositions and the natrocarbonatite lavas at Lengai has been suggested by various authors (Williams et al., 1986; Peterson, 1989b, 1990; Lee and Wyllie, 1994; Bell and Dawson, 1995; Keller and Spettel, 1995; Church and Jones, 1995; Kjarsgaard et al., 1995; Dawson et al., 1996; Simonetti et al., 1997; Dawson, 1998; Lee and Wyllie, 1998). The exact composition of conjugate silicate and carbonatite liquids, and the moment and conditions of separation of the two melts is still a matter of discussion.

Models for the evolution of the Lengai suite from parental mantle melts invoke derivation from high magnesian olivine nephelinites and olivine melilitites (Peterson and Kjarsgaard, 1995; Dawson, 1998). Peterson (1989b) argues that olivine nephelinites evolve by fractionation towards mildly peralkaline nephelinites and associated calciocarbonatites, as at Shombole volcano, Kenya, whereas at Lengai the parental magma is thought to be melilititic, and the fractionation is directed towards highly peralkaline combeite–wollastonite nephelinites (CWN). From these, natrocarbonatite exsolves in the final stage of the evolution. The hypothetical melilitite parent of Peterson is derived from the tuff cones of the northern and eastern foreland of Lengai and Kerimasi (Fig. 1). This paper focuses in particular on *high-Mg* olivine melilitites at Oldoinyo Lengai itself and compares these to similar lavas in the surroundings of the volcano. Whatever the exact composition of primary mantle melts at Oldoinyo Lengai is, there remains a large compositional gap between these and the evolved phonolites and peralkaline nephelinites of the Lengai I and Lengai II stages of the cone.

3. Occurrence of melilititic rocks at and around Oldoinyo Lengai

Melilititic rocks have been described from the tuff cone field on the floor of the rift valley between Engaruka and Lake Natron, thus in the wider area around Oldoinyo Lengai (Dawson and Powell, 1969; Dawson et al., 1985; Peterson and Kjarsgaard, 1995; Johnson et al., 1997). In volcanic rocks directly related to the Lengai cone, melilite has been found in spherical lapilli and ashes related to the explosive paroxysms between periods of effusive natrocarbonatitic activity (Dawson et al., 1968; Hay, 1989; Keller and Krafft, 1990; Dawson et al., 1992). The melt component of these lapilli and ashes crystallised as highly evolved melilite-bearing nephelinites, with nepheline, aegerine–augite, melanite–schorlomitic garnet, titanite, melilite, wollastonite and combeite. They are thus closely related to the combeite–wollastonite nephelinite lavas, the CWN group of the more recent Lengai. The melilite composition in these evolved Oldoinyo Lengai rocks is

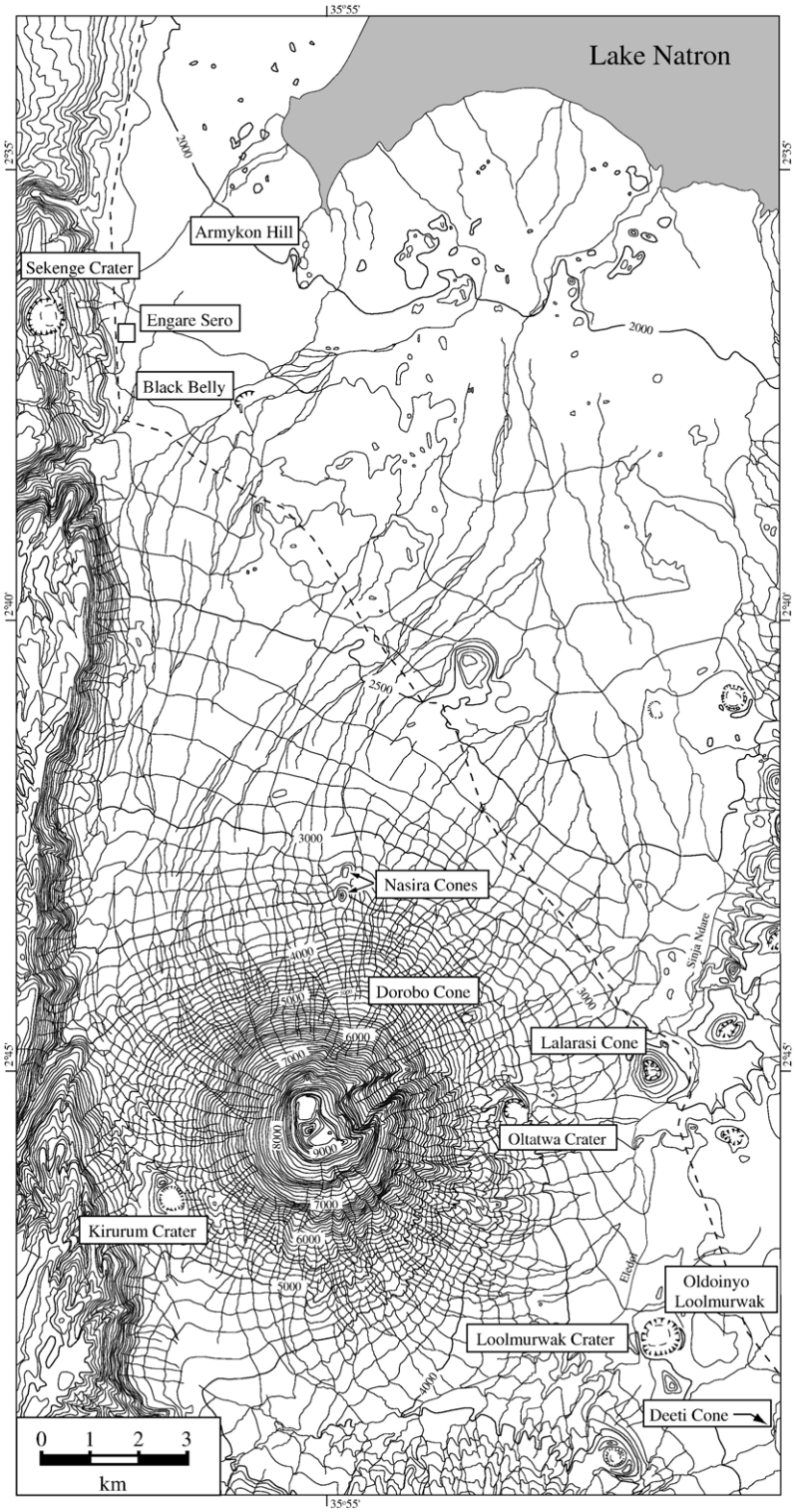

Fig. 1. Map of the Natron-Oldoinyo Lengai area, showing craters and cones. Topography adapted from Sheet 39/4 Topographic Map series 1:50,000.

unusual compared to the field of magmatic melilite of Velde and Yoder (1977). They are also distinct from melilite in olivine melilitites due to their higher Fe and Na contents (Keller and Krafft, 1990; Peterson and Kjarsgaard, 1995; Dawson, 1998; Wiedenmann, 2004).

Fig. 1 shows the location of minor volcanic centres around Oldoinyo Lengai. These cones and craters of olivine melilititic lava composition form the essential basis for the present work: Armykon Hill at the southern shore of Lake Natron, Lalarasi Cone on the eastern foot of Oldoinyo Lengai, and the newly described Dorobo Cone and Kirurum Crater. The latter two are parasitic centres on the slopes of Lengai and stratigraphically interlayered with the products of recent Lengai activity. Other centres such as Sekenge and Oltatwa Craters (Fig. 1) have not been described before. Sekenge Crater is carved into the alkali-basaltic and nephelinitic lava sequence of the rift escarpment above Engare Sero village. Embalulu Oltatwa–Oltatwa Crater–is the parasitic centre on the eastern slope of Oldoinyo Lengai, shown but not named on the map of Dawson (1962). Both centres have only produced pyroclastics that are classified as biotite–megacrystic olivine melilitites (Wiedenmann, 2004; Finkenbein, 2005). Black Belly or "Norok Nokoschoke" is a flat tuff ring about 3 km SSW of Armykon Hill between Oldoinyo Lengai and Lake Natron. Its bedded pyroclastic sequence carries olivine melilitites as juvenile components, but no lava flows. Also several small, unnamed olivine melilitite cinder or lapilli cones are present in the area between Sinja River-Lalarasi and the eastern flank of Oldoinyo Lengai. Small grain size, admixture of xenocrysts and secondary alteration of glass and melilite renders a quantitative chemical characterisation of the magmatic components of these pyroclastic centres generally difficult.

Most of the numerous Engaruka-Natron tuff cones and centres of Dawson and Powell (1969) have not been explored and described in any detail. Loolmurwak Crater and the olivine–melilite nephelinites of Oldoinyo Loolmurwak are referred to in Dawson et al. (1985) and Hay (1983). Johnson et al. (1997) have described a suite of mantle xenoliths from Deeti tuff cone (Fig. 1) and define the host magma as olivine poor, mica porphyritic melilitite. Pello Hill, Eledoi and Loluni craters are renowned xenolith localities (Dawson and Smith, 1988; Johnson et al., 1997; Lee et al., 2000). The magmatic component of Pello Hill, derived from a quite altered host scoria, is given as potassic olivine nephelinitic or melilititic (Dawson and Smith, 1988; Johnson et al., 1997). It thus appears that most of the tuff cones are of mica-porphyritic melilite nephelinite composition, with the most pronounced olivine melilitites in the immediate Oldoinyo Lengai area.

A direct co-magmatic relationship between the melilititic-nephelinitic tuff cones on the rift floor and the volcanic evolution of Oldoinyo Lengai has previously been suggested (Dawson et al., 1985; Peterson and Kjarsgaard, 1995; Johnson et al., 1997), but here we present evidence that the parasitic centres on the slopes of Lengai itself (Fig. 1) are melilititic and are intimately related to the volcanic sequence of the main cone of Oldoinyo Lengai. These specific centres are Dorobo Cone (DC), Armykon Hill (AH) and Sinja Lalarasi (SL) and are the focus of this study on possibly primary magmas. Therefore, a short description of field occurrence and relationship to Oldoinyo Lengai follows (Fig. 1).

3.1. Armykon Hill

Armykon Hill, at the south shore of Lake Natron, is a tuff ring with large olivine melilititic bombs and blocks in bedded pyroclastics. Dawson et al. (1985) have given a composition which shows a moderately fractionated olivine melilitite similar to OL 12/99 in Table 1. Black glassy lava flows (OL 12/2K in Table 1; Fig. 2) extend southwards from the cone and the dissected east flank of Armykon Hill exhibits a large body of olivine melilitite as a very shallow intrusion or a solidified lava lake (OL 336). In this sample, olivine is partly rimmed by monticellite.

3.2. Lalarasi Cone

A prominent steep cone, about 200 m high and with a well preserved double-crater on its top, dominates the eastern foot of Lengai close to the river bed of Sinja Eledoi/Sinja Ndare and directly on the track from Engaruka to Lake Natron. This cone is known as Lalarasi in the literature and this name figures also on published topographic and geological maps (Dawson, 1962; Map Series 1:50,000 Sheet 39/4 Oldoinyo Lengai). Although all our local guides insisted that the name Lalarasi refers to another hill about 9 km to the NW we will keep the name Lalarasi as introduced in the geological literature. The first reference to this cone by Reck (1914) calls this volcano "Sinja Krater". Therefore, when the necessity for distinction occurs, we will use "Sinja Lalarasi (SL)" for this volcano at 35°58.6′E, 02°45′S. The Sinja Lalarasi cone is made up of melilitite lapilli beds with the typical spherical lapilli and spherical bombs that are highly characteristic for the

Table 1
Major and trace element analyses of the olivine melilitites and glass matrix of OL 12 from Armykon Hill

Unit	Dorobo Cone Oldoinyo Lengai			Armykon Hill Lake Natron				Lalarasi Sinja Eledoi		Oldoinyo Loolmurwak olivine–melilite nephelinite			Kirurum Crater
Sample	OL 198	OL 198B	OL 343	OL 336	OL 12/99	OL 12/2K	OL 12Gl	OL 350	OL 352	OL 199	OL 342	OL 141	OL293C
wt.%													
SiO_2	36.48	36.52	36.35	33.71	34.14	34.07	44.75	34.35	36.38	38.31	38.06	38.26	32.50
TiO_2	4.25	4.57	4.49	5.77	5.80	5.83	2.99	5.20	4.27	3.93	3.75	3.79	4.34
Al_2O_3	7.52	7.08	7.12	7.24	7.03	6.92	12.96	7.39	7.51	7.22	7.25	7.26	7.48
Fe_2O_3	5.69	6.40	14.60*	15.43*	7.90	5.74	8.90*	15.52*	14.19*	7.65	14.56*	6.16	15.08*
FeO	7.78	7.68			6.91	8.80				6.39		8.01	
MnO	0.22	0.21	0.20	0.23	0.23	0.22	0.21	0.24	0.21	0.20	0.21	0.21	0.28
MgO	13.78	15.11	15.04	9.58	9.85	9.80	2.58	9.93	14.92	15.38	14.59	15.30	7.10
CaO	14.28	14.00	13.52	16.96	16.71	16.47	1.73	17.66	13.47	12.88	13.11	13.44	20.29
Na_2O	4.20	3.09	3.64	4.40	4.28	5.30	12.27	3.75	3.48	2.67	2.67	2.19	4.47
K_2O	2.53	2.18	2.36	2.70	2.59	3.08	9.22	2.21	2.36	1.48	1.74	1.36	2.26
P_2O_5	1.01	0.96	0.95	1.34	1.51	1.56	0.79	1.22	0.89	0.91	0.90	0.89	1.15
CO_2	0.16	0.20	0.20	0.26	0.26	0.29	n.a.	0.10	0.44	0.11	1.52	0.18	2.50
SO_3	0.22	0.20	0.10	0.09	0.21	0.32	1.11	0.04	0.11	0.05	b.d.l.	0.09	0.18
Cl	0.05	0.01	0.03	0.09	0.02	0.18	0.71	b.d.l.	0.06	0.01	b.d.l.	b.d.l.	0.06
F	0.24	0.20	0.12	0.47	0.25	0.30	0.54	0.40	0.10	0.09	0.11	0.07	0.20
H_2O	0.91	1.01	0.74	0.12	1.20	0.29	n.a.	0.41	0.26	1.59	1.31	2.00	2.85
–O=F, Cl	0.11	0.09	0.06	0.22	0.11	0.17	0.39	0.17	0.06	0.04	0.05	0.03	0.10
Total	99.21	99.33	99.40	98.17	98.78	99.00	98.36	98.25	98.59	98.83	99.73	99.18	100.64
Mg#	68.7	69. 6	69.8	58.3	58.7	58.7	39.4	59.0	70.3	70.1	69.3	69.5	51.4
AI	1.28	1.05	1.20	1.40	1.40	1.74	2.33	1.16	1.10	0.83	0.87	0.70	1.31
ppm	#	#	×	×	×	#	##	×	×	#	×	×	#
Cs	0.70	0.45	n.a.	n.a.	n.a.	0.71	n.a	n.a.	n.a.	0.26	n.a.	n.a.	0.22
Rb	59.6	55.5	51	49	54	61.2	71	49	51	37.1	42	36	39.4
Sr	1501	1260	1121	1427	1579	1479	368	1364	1189	973	1087	1672	1785
Ba	956	774	983	1103	919	908	1552	1257	1168	673	780	747	1061
Pb	6.49	6.22	7	12	7	8.78	4.77	9	6	5.3	6	7	9.04
Y	28.6	24.3	31	44	55	36.6	21.6	43	29	28.1	33	34	36.2
Nb	123	111	123	158	153	167	103	156	118	101	104	99	180
Zr	370	418	377	576	605	567	845	454	349	395	373	369	515
Hf	8.11	7.43	8	11	12	12.7	16.06	9	7	8.2	8	9	11
V	311	347	274	311	289	375	236	337	264	300	228	265	133
Sc	25	26	35	39	29	30	30	37	34	22	27	26	29
Ni	300	307	350	104	139	128	9.9	89	296	368	374	399	12.2
Cr	607	615	599	110	161	218	b.d.l.	112	481	722	620	654	b.d.l.
Co	67.7	63.8	73	49	50	57.1	7.4	50	67	69.5	71	70	45.3
Cu	162	152	172	191	247	197	n.a.	232	176	126	131	127	276
Zn	147	125	124	106	140	167	42	132	119	142	133	131	159
Ga	19.9	16.8	17	20	17	21.8	n.a.	16	16	19.4	17	15	18.1
Th	11.3	10.2	7	8	b.d.l.	13.5	b.d.l.	11	6	10	5	<5	5.14
U	3.03	2.52	<3	<3	<5	3.63	1.68	<3	<3	2.53	<3	<5	4.01
Ta	7.66	7.51	10	7	<5	11.9	1.18	6	8	7.19	8	<5	7.93
Be	3.8	3.0	n.a.	n.a.	n.a.	4.62	n.a.	n.a.	n.a.	3.02	n.a.	n.a.	5.09

OL12Gl: glass matrix, major elements by SEM/EDS; *: total iron; Mg#: $Mg/(Mg+Fe^{2+})$ ($Fe_2O_3/FeO=0.15$); AI: peralkalinity index $(K+Na)/Al$; ×: trace elements by XRF; #: trace elements by ICP-MS; ##: trace elements by LA ICP-MS; b.d.l.: below detection limit; n.a.: not analyzed.

very fluid melilititic melts of the area. Also a general feature is the strong alteration of melilite that characterises most similar deposits of the area and renders these pyroclastics completely unsuitable for bulk rock geochemistry.

Dawson et al. (1985) report an olivine melilititic lava flow about 1.5 km north of the Sinja Lalarasi cone and refer to this as the Lalarasi flow. The Lalarasi flow of Dawson et al. (1985) is exposed at 35°59.16′E, 02°43.80′S at the exit of the Sinja Eledoi/Sinja Ndare canyon which is carved into debris avalanche deposits (DADs) of one of the major collapse events that affected the younger history of Oldoinyo Lengai cone (Keller, 2002; Klaudius and Keller, 2004). Klaudius and Keller (2006-this issue) obtained a C-14 age of ca. 2500 years B.P. for this collapse event on embedded plant remains. Olivine melilititic units occur before (Lalarasi flow, OL 350 in Table 1) and directly following the collapse (lava blocks in an olivine melilitite breccia, OL 352). According to these geological relationships, the DAD age can be used as a guide to the approximate age for the Lalarasi melilitites.

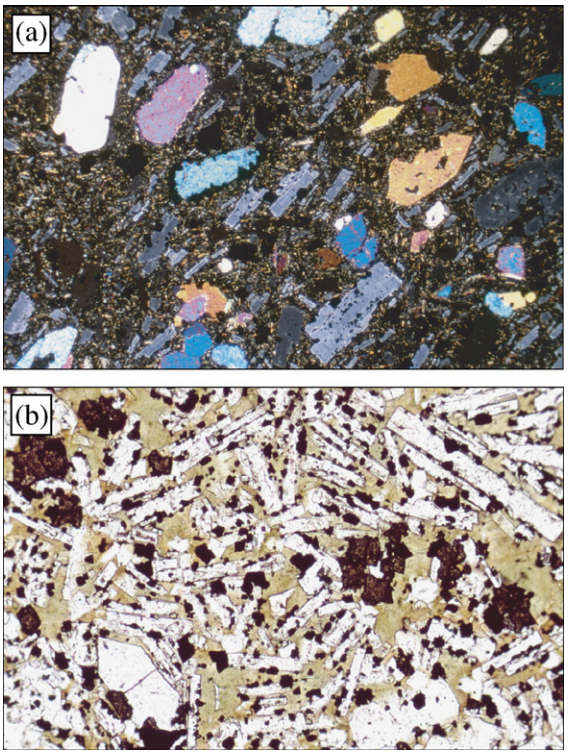

Fig. 2. Thin section photographs of olivine melilitite. (a) Olivine-rich melilitite OL 198 from Dorobo Cone. P+, width of photograph 5 mm. (b) Olivine–melilitite OL 12/2K with green-glass matrix from Armykon Hill, dark brown mineral is perovskite. PPL, width of photograph 1.4 mm.

3.3. Dorobo Cone

The Dorobo parasitic cone of Oldoinyo Lengai lies on the south-eastern slope at an elevation of 1200–1250 m (35°56.6′E, 02°44.4S). The name refers to its position on the eastern climb track to the summit of Oldoinyo Lengai that was pioneered by the Dorobo organisation of Arusha (Nyamweru, 1988; Dawson in SEAN, 1988; Keller and Krafft, 1990). From most sides the hill is not very pronounced, but morphologically it is a well-preserved tuff cone with a breached horseshoe crater. No local name is available although some of our Maasai sources called it "Larbenne". Along the southern side of the Dorobo Cone, the Dorobo canyon descends in an NE direction providing important stratigraphic sections for the relationship between the Dorobo Cone and Oldoinyo Lengai. Fresh and dense primitive olivine melilitite occurs as blocks up to 20 cm in diameter in a debris-flow unit descending from the cone. These Dorobo olivine melilitites, first described in this paper, play an important role in our discussions because of (i) their clear relationship to the cone of Oldoinyo Lengai, and (ii) due to their primitive compositions with high MgO, Ni and Cr contents as compared to Armykon Hill, and to Dawson's Lalarasi flow, and to the more fractionated compositions at the Kirurum parasitic crater.

The Dorobo Cone itself is also of particular volcanological interest forming a thick near-vent accumulation of melilitic Pele's tear-drop lapilli, exposed in a 40–50 m section of well bedded lapilli tuffs. The lapilli are juvenile magmatic components, generally up to 1–2 cm in diameter; they are glassy and vesicular. The lapilli have undergone intense carbonatisation with calcite contents of up to 40 vol.% replacing melilite and glass to varying degrees. Their low Ni and Cr contents (<10 ppm) and the seemingly olivine-free original composition suggest an evolved melilititic composition. Petrographically similar, also extensively carbonatised gray melilitite lava flows are exposed in the canyon at the foot of the cone. This process of intense carbonate alteration is specific to the evolved Dorobo melilitites and is not observed in this form in phonolitic and nephelinitic pyroclasts with which they are interlayered. It may indicate a high CO_2 content in the evolved melilitite melt. In contrast to these carbonated evolved melilitites, the olivine melilitite samples analyzed in this paper are generally fresh and unaltered (Fig. 2, Table 1).

The Dorobo sequence–droplet lapilli-tuffs, carbonated melilitite lava, and debris-flow deposits with angular blocks of primitive olivine melilitite lava–overlies Bi–Ol–Cpx tuff breccias of Unit II of Dawson (1962). It is covered by yellow nephelinitic breccias of young debris-avalanche deposits (DADs, Klaudius and Keller, 2004). Two radiocarbon dates from plants incorporated into the base of the Dorobo pyroclastics give an age of ca. 3000 and 2500 years B.P., respectively. Details of this first C-14 dating at Oldoinyo Lengai will be presented elsewhere. It is, however, worth noting that this coincides with the age of the Sinja-Lalarasi olivine melilitites, thus pointing to a general olivine melilititic activity at Oldoinyo Lengai around this period.

3.4. Kirurum Crater

Embalulu Kirurum, the Kirurum Crater, is the prominent elliptical crater on the SW flank of Oldoinyo Lengai located in the saddle towards the rift escarpment. The morphologically young crater is carved into material of Lengai I and more recent Lengai products, but also covered by nephelinites of the CWN group.

The crater walls exhibit thick accumulations of olivine melilititic lapilli tuffs. A major unit forming the 120 m thick northern deposition apron of the crater is dominantly composed of monolithologic glassy lapilli

in teardrop shapes. Melilite forms the essential mineral, with varying olivine contents. As generally observed, pyroclastics and individual lapilli are much more affected by secondary alteration than lava samples. Nevertheless, a larger juvenile clast could be analyzed and serves in the following discussion as an example for fractionated olivine melilitites (OL 293 in Table 1).

3.5. Loolmurwak crater group

The Loolmurwak crater group on the south-eastern foot plain of Oldoinyo Lengai, between Oldoinyo Lengai and Kerimasi (Dawson and Powell, 1969; Hay, 1983; Dawson et al., 1985; Johnson et al., 1997), consists of 3 volcanic edifices. These are part of a wider field including Kisete Crater and Deeti Tuff Cone to the south and form part of the Engaruka-Natron tuff cones of Dawson and Powell (1969). The spectacular Loolmurwak explosion crater with its diameter of almost 1 km and nearly vertical walls of over 100 m height has emitted melilititic Ol–Bi–Cpx tuffs and exposes carbonatitic pyroclastics in its lower inner walls. These are attributed by Hay (1983) to Kerimasi. An elongated tuff cone, about 70 m high, extends SE from Loolmurwak crater and consists of melilite–nephelinite lapilli and scoriae. The broad volcanic hill of Oldoinyo Loolmurwak itself lies east of the crater pit (Fig. 1). The Loolmurwak flow of Dawson et al. (1985) is a lava from its southern side. We report in Table 1 the composition of a lava flow from the eastern side of Loolmurwak, a flow from the southern side and of a lava block from pyroclastics on its north-western tip. As will be shown, these Loolmurwak olivine–melilite nephelinites are compositionally distinct from the olivine melilitites with a more direct relationship to Oldoinyo Lengai.

3.6. Nasira crater row

The only prominent exception from the generally melilititic nature of the young parasitic centres of Oldoinyo Lengai is given by the north–south directed row of three morphologically very youthful Strombolian cones on the lower north slope of Lengai. The name for these cones was indicated to us by the local Maasai as “Nasira”, hence “Nasira Craters” in Fig. 1. Dawson (1962) mentions these craters and groups them under his Melanephelinitic Extrusives, but defines them later (Dawson, 1998) as wollastonite nephelinite (sample WN 4421). The composition of the magmatic components (lapilli, scoriae, spherical bombs—often cored by ijolitic plutonic cumulates), and of a short lava flow emitted from the middle cone of the row are black glass-rich, in part melilite-bearing combeite–wollastonite nephelinites belonging mineralogically and chemically to the CWN group of Lengai II (Klaudius and Keller, 2006-this issue).

4. Composition of olivine melilitites

4.1. Analytical techniques

A description of analytical techniques is found in the appendix.

4.2. Petrography of olivine melilitites

All olivine melilitites are highly porphyritic volcanic rocks with olivine and melilite as the major phenocryst and microphenocryst phases. Perovskite and opaque spinel group minerals occur as phenocrysts and microphenocrysts up to 200 μm with a few megacrystic grains found up to 5 mm in diameter. Clinopyroxene is not a common phase in olivine melilitites, although sparse phenocrysts are found. Only the Oldoinyo Loolmurwak olivine–melilite nephelinite (OL 141, 191, 342) has clinopyroxene as an important microphenocryst and groundmass phase. Other components of olivine melilitites are nepheline as rare microphenocrysts in the interstitial matrix, and sparse schorlomitic garnet.

In the following section on mineral chemistry two particular occurrences are analyzed and compared. (1) Samples from the Dorobo Cone (OL 198, 198B, 343) represent the most magnesian variety with whole rock Mg# of 70; (2) the Armykon Hill lavas (OL 12, 12/2K, 336) are representatives for the slightly more evolved olivine melilitites as on Armykon Hill and the Lalarasi flow, with Mg# ≤ 60 (Table 1). The two groups in Table 1–primitive with MgO 14–15 wt.%, and more evolved with MgO <10 wt.%–differ mainly in their relative contents of olivine and melilite phenocrysts. The few analyses in the literature (Dawson et al., 1985) cover only the more evolved variety from Armykon Hill and the Lalarasi flow. This paper adds the group of high-Mg olivine melilitites of Dorobo Cone and Lalarasi to the discussion and relates Dorobo Cone, Lalarasi Cone and Armykon Hill directly to the evolution of Oldoinyo Lengai. In contrast, the Oldoinyo Loolmurwak olivine–melilite nephelinites are compositionally distinct and relate to the wider field of craters and tuff cones between Engaruka and Gelai volcano (Dawson and Powell, 1969; Johnson et al., 1997). Lava flows of Armykon Hill show a flow-

Table 2
Rare earth element data for olivine melilitites

Location	Dorobo Cone		Oldoinyo Loolmurwak	Armykon Hill		Kirurum Crater
Sample	OL 198B lava block	OL 198 lava block	OL 199 lava block	OL 12/2K lava flow	OL 12/2K glass matrix	OL 293C lava block
ppm						
La	84.9	95.3	83.1	124	6.35	100
Ce	165	180	167	249	5.50	165
Pr	19.1	20.5	19.7	29.3	0.48	18.2
Nd	75.5	76.5	77	114	1.89	67
Sm	12.7	13.5	14	19.9	0.78	13.4
Eu	3.8	3.94	4.09	5.99	0.41	4.23
Gd	9.41	9.66	9.98	15.1	1.85	11.2
Tb	1.24	1.25	1.37	1.83	0.36	1.52
Dy	5.85	6.3	6.62	9.04	2.89	7.48
Ho	0.892	0.972	0.975	1.34	0.65	1.2
Er	2.07	2.29	2.32	3.11	1.97	2.82
Tm	0.145	0.274	0.297	0.372	0.30	0.366
Yb	1.34	1.66	1.59	2.11	1.97	2.09
Lu	0.187	0.232	0.228	0.281	0.30	0.317

REE data by ICP-MS; REE data for OL 12/2K glass matrix by LA ICP-MS.

surface facies of olivine melilitite with a spectacular green glassy matrix (Fig. 2); due to crystallisation of olivine, melilite, perovskite and spinel group minerals, this glass is strongly depleted in MgO, CaO, TiO_2 and REE (Tables 1 and 2).

4.3. Mineral chemistry

Selected representative analyses of minerals from olivine melilitites are given in Table 3. See Supplementary Tables 5–13 and Supplementary Figs. 13 and 14 in Appendix A for additional data on mineral chemistry.

4.3.1. Olivine

Microprobe data of olivine are listed in Table 3 and Supplementary Table 5. Representative compositions of olivine from this study (Armykon Hill and Dorobo Cone) are plotted, together with available published data (Dawson et al., 1985), in terms of Fo vs. NiO in Supplementary Fig. 13. Forsterite contents show a relatively small range between Fo 88–81, with the lowest value in olivine from a crystallised melt inclusion (Dorobo OL 198) and the highest value from a phenocryst rim in the same sample. Lower Fo values (maximum Fo 76) are reported by Dawson et al. (1985) for olivine in the Loolmurwak olivine–melilite nephelinite. Phenocrysts from Armykon Hill lava show a zonation from Mg-rich cores (Fo 86–85) to Fe-enriched rims (Fo 85–84). This is accompanied by decreasing NiO and increasing CaO contents from core to rim with 0.32–0.38 to 0.06–0.17 wt.% NiO and 0.16–0.21 to 0.42–0.87 wt.% CaO, respectively. Core and rim compositions of microphenocrysts are relatively homogeneous in terms of Fo content and show similar core–rim behaviour for Ni and Ca.

In contrast, the olivine from samples of the Dorobo parasitic cone has a more complex pattern of both normal and reverse zoning. Phenocrysts have generally Mg-rich cores and Fe-rich rims (Fo 87 to Fo 85), with some grains showing opposite trends, e.g. Fo 81 to 88 in a core to rim traverse. Most microphenocrysts have Fe-enriched cores and Mg-enriched rims with Fo values of 84 and 86, respectively. Dawson et al. (1985) have also documented reverse zonation for olivine from Lalarasi olivine melilitites.

NiO contents in the Dorobo olivine are high and attain 0.46 wt.% in Mg-rich cores of the phenocrysts. Reversely zoned phenocrysts show slight enrichment in NiO towards the rims, e.g. 0.19 and 0.25 wt.% in a core to rim traverse. Neither optical microscopy nor BSE imaging reveal any resorption features (Fig. 3a).

Supplementary Table 6 lists trace-element contents in the Armykon Hill olivine, analyzed by LA ICP-MS. In addition to Ni, Mn, Cr, Co and Zn as minor components, traces of Sc, V, Zr and Y have been analyzed. Other elements are below detection limits (less than 0.05–0.1 ppm). Phenocrysts have higher Ni (up to 2307 ppm), Cr (up to 188 ppm), Co (up to 128 ppm) and Zn (up to 102 ppm) compared to microphenocrysts, which contain more Mn (up to 1937 ppm). Sc, Y and Zr are slightly higher in

Table 3
Selected analyses of minerals from olivine melilitites

Mineral	Olivine				Melilite				Nepheline	Clinopyroxene			Garnet	Spinel			Perovskite			
Sample	OL 198		OL 12		OL 198		OL 12		OL 198	OL 198B			OL 198	OL 198			OL 198		OL 12	
	Phenocryst		Phenocryst		m-phenocryst		Phenocryst		Phenocryst	Phenocryst			Phenocryst	Phenocryst			Euhedral		Round	
	Core	Rim	Core	Rim	Core	Rim	Core	Core	Core	Core	Core	Rim	Rim	Core	Mantle	Rim	Core	Rim	Core	Rim
wt.%																				
SiO_2	40.22	39.23	40.11	39.19	42.90	43.13	43.27	43.29	40.34	50.81	51.38	48.31	24.24	0.25	0.23	0.32	b.d.l.	b.d.l.	b.d.l.	b.d.l.
TiO_2	b.d.l.	0.04	0.04	0.03	0.07	0.06	0.05	0.05	b.d.l.	0.31	0.55	2.66	18.77	3.94	13.86	17.65	57.40	57.02	57.22	57.31
Al_2O_3	b.d.l.	b.d.l.	0.03	b.d.l.	4.56	5.32	4.15	3.85	32.01	0.62	0.86	4.79	0.31	11.75	2.69	1.68	b.d.l.	b.d.l.	b.d.l.	b.d.l.
Fe_2O_3*					0.19	0.41	1.38	0.57	3.02	8.30	5.04	3.66	20.86	12.75	33.57	35.01	1.10	1.15	1.11	1.31
FeO*	12.24	14.53	13.09	14.85	3.01	3.16	2.41	2.90		11.56	10.58	2.84	1.83	21.51	33.74	38.24				
MnO	0.17	0.21	0.19	0.25	0.05	0.06	0.06	0.07	n.a.	0.62	0.46	0.13	0.41	0.35	0.67	0.72	b.d.l.	b.d.l.	b.d.l.	b.d.l.
MgO	47.23	45.79	45.92	44.04	9.46	8.73	9.74	9.83	b.d.l.	5.83	8.86	13.44	1.09	9.61	6.32	5.17	b.d.l.	b.d.l.	b.d.l.	b.d.l.
CaO	0.15	0.43	0.16	0.53	35.53	34.43	36.40	36.15	0.52	18.47	21.09	24.49	31.72	b.d.l.	b.d.l.	0.28	39.29	39.93	40.12	40.20
Na_2O	b.d.l.	b.d.l.	b.d.l.	b.d.l.	2.44	3.04	2.39	2.27	12.73	3.19	1.74	0.40	0.30	n.a.	n.a.	n.a.	0.46	0.29	0.37	0.36
K2O	n.a.	n.a.	n.a.	n.a.	0.15	0.19	0.15	0.16	11.61	n.a.	n.a.	n.a.	n.a.	n.a.	n.a.	n.a.	n.a.	n.a.	n.a.	n.a.
V_2O_3	n.a.	n.a.	n.a.	n.a.	n.a.	n.a.	n.a.	n.a.	n.a.	n.a.	n.a.	n.a.	0.45	0.24	0.42	0.52	n.a.	n.a.	n.a.	n.a.
Cr_2O_3	n.a.	n.a.	n.a.	n.a.	n.a.	n.a.	n.a.	n.a.	n.a.	b.d.l.	b.d.l.	b.d.l.	n.a.	38.25	8.10	b.d.l.	n.a.	n.a.	n.a.	n.a.
NiO	0.43	0.23	0.32	0.06	n.a.	n.a.	n.a.	n.a.	n.a.	n.a.	n.a.	n.a.	n.a.	n.a.	n.a.	n.a.	n.a.	n.a.	n.a.	n.a.
SrO	n.a.	n.a.	n.a.	n.a.	n.a.	n.a.	n.a.	n.a.	n.a.	n.a.	n.a.	n.a.	n.a.	n.a.	n.a.	n.a.	0.24	0.19	0.24	0.25
ZrO_2	n.a.	n.a.	n.a.	n.a.	n.a.	n.a.	n.a.	n.a.	n.a.	n.a.	n.a.	n.a.	0.62	n.a.	n.a.	n.a.	b.d.l.	0.06	b.d.l.	0.05
Nb_2O_3	n.a.	n.a.	n.a.	n.a.	n.a.	n.a.	n.a.	n.a.	n.a.	n.a.	n.a.	n.a.	n.a.	n.a.	n.a.	n.a.	0.28	0.41	0.15	0.22
La_2O_3	n.a.	n.a.	n.a.	n.a.	n.a.	n.a.	n.a.	n.a.	n.a.	n.a.	n.a.	n.a.	n.a.	n.a.	n.a.	n.a.	0.32	0.24	0.28	0.26
Ce_2O_3	n.a.	n.a.	n.a.	n.a.	n.a.	n.a.	n.a.	n.a.	n.a.	n.a.	n.a.	n.a.	n.a.	n.a.	n.a.	n.a.	0.98	0.58	0.66	0.48
Pr_2O_3	n.a.	n.a.	n.a.	n.a.	n.a.	n.a.	n.a.	n.a.	n.a.	n.a.	n.a.	n.a.	n.a.	n.a.	n.a.	n.a.	0.11	0.05	b.d.l.	b.d.l.
Nd_2O_3	n.a.	n.a.	n.a.	n.a.	n.a.	n.a.	n.a.	n.a.	n.a.	n.a.	n.a.	n.a.	n.a.	n.a.	n.a.	n.a.	0.48	0.22	0.35	0.24
ThO_2	n.a.	n.a.	n.a.	n.a.	n.a.	n.a.	n.a.	n.a.	n.a.	n.a.	n.a.	n.a.	n.a.	n.a.	n.a.	n.a.	0.07	b.d.l.	0.16	0.10
UO_2	n.a.	n.a.	n.a.	n.a.	n.a.	n.a.	n.a.	n.a.	n.a.	n.a.	n.a.	n.a.	n.a.	n.a.	n.a.	n.a.	0.06	b.d.l.	b.d.l.	b.d.l.
Total	100.44	100.46	99.86	98.95	98.36	98.53	100.00	99.68	100.23	99.71	100.57	100.72	100.60	98.65	99.60	99.59	100.77	100.13	100.66	100.78

OL 198 and 198B: Dorobo Cone; OL 12: Armycon Hill.
m-phenocryst: microphenocryst; *: for olivine all Fe as FeO, for nepheline and perovskite all Fe as Fe_2O_3, for melilite, clinopyroxene, garnet and spinel Fe_2O_3 and FeO calculated from charge balance; b.d.l.: below detection limit; n.a.: not analyzed.

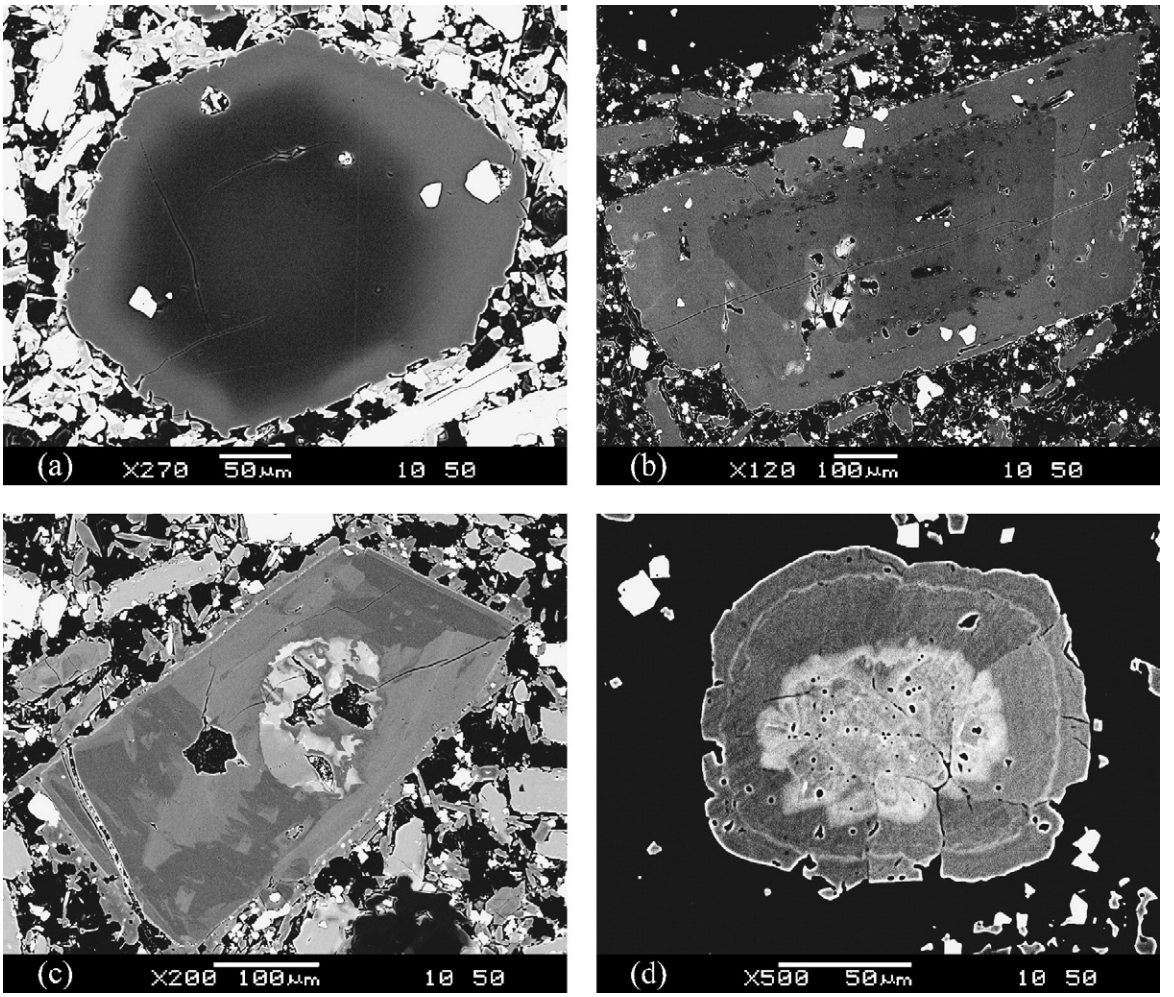

Fig. 3. Backscattered electron (BSE) images showing (a) zoned olivine phenocryst surrounded by melilite microphenocrysts (OL 198), (b) zoned melilite phenocryst surrounded by melilite microphenocrysts (OL 198), (c) zoned green-core clinopyroxene phenocryst surrounded by melilite microphenocrysts (OL 198B), (d) zoned perovskite (OL 198B).

microphenocrysts, and phenocrysts are slightly enriched in V. In general, core–rim variations in both pheno- and microphenocrysts show highest Ni, Cr, Co and Zr in cores and elevated Mn in rims.

The complex zoning pattern observed in particular in the high-Mg Dorobo olivine melilitites indicates repeated changes of crystallisation conditions (e.g. Dunworth and Wilson, 1998).

4.3.2. Melilite

Melilite is a major phenocrystic mineral phase in olivine melilitites, but few chemical data are available. Dawson et al. (1985) published two analyses of melilite from Armykon Hill and Lalarasi. Representative analyses of melilites from Dorobo Cone and from Armykon Hill are listed in Table 3 and Supplementary Table 7, and are plotted in Supplementary Fig. 14 in terms of their $Ca_2MgSi_2O_7$, $Ca_2FeSi_2O_7$ and $CaNaAlSi_2O_7$ end-member compositions. Melilite from both localities exhibit a relatively narrow range in composition, characterised by high MgO (8.6–9.9 wt. %) with subordinate Al_2O_3 (3.9–5.9 wt.%), low Na_2O (2.3–3.3 wt.%) and FeO (2.7–3.7 wt.%). The melilite compositions from olivine melilitites are thus classified as sodium åkermanite. Melilite from the crystallised melt inclusions contains the highest FeO of 4.5 wt.% and the lowest MgO of 8.4 wt.% for melilite in olivine melilitites. Most of the melilite phenocrysts and microphenocrysts are unzoned. Only one phenocryst in the Dorobo sample OL 198B has a core slightly enriched in Na and Al and depleted in Mg and Fe compared to the rim (Fig. 3b; Supplementary Table 7).

Melilite is also a prominent constituent in the younger silicate rocks of Oldoinyo Lengai, in particular the pyroclastic sequences of historic and pre-modern eruptions where the magmatic components are spherical lapilli of melilite-bearing nephelinites. This melilite of the evolved silicate rocks has unusual compositions extending the field of magmatic melilite of Velde and Yoder (1977) considerably. This is best seen in their high Fe and Na contents (Dawson et al., 1989; Keller and Krafft, 1990). Compared to the olivine melilitites, melilite from evolved Oldoinyo Lengai rocks is Fe- and Na-rich (up to 10.3 wt.% and 8.2 wt.% oxides respectively), has Al_2O_3 up to 8.0 wt.% and lower MgO (3.2–7.0 wt.%). In end-member composition this results in high $CaNaAlSi_2O_7$ contents and unusually high birefringence under the microscope (Keller and Krafft, 1990; Wiedenmann, 2004).

Trace element concentrations were obtained by LA ICP-MS analyses of melilite phenocryst from Armykon Hill (Supplementary Table 8). These show Sr as a major trace element in melilite with the highest concentration of 3220 ppm. Ti and Mn are in the range of 350–430 ppm and Zn varies between 170 and 230 ppm. Lower concentrations have been obtained for Ba (45–52 ppm), Co (29–34 ppm) and Ni (12–14 ppm). Sc, V and Y are present in amounts of 2.6–3.7 ppm, while Pb, Zr and Rb are <1 ppm. Rare earth elements (REE) have been found in åkermanite with concentrations between 46.7 and 48.6 ppm, with the highest contents for La and Ce of 11.8–14.1 ppm and 17.1–19.6 ppm, respectively. The results show that Sr is the most important trace element in melilite, and melilite in olivine melilitites is not a carrier for the REE. No core-to-rim variations have been found for those concentrations of trace elements in melilite.

In summary, melilite from olivine melilitites has the most "primitive" composition compared to other Lengai rocks; it is also similar to melilite from other olivine melilitites, e.g. from SW Germany (Keller et al., 1990; Dunworth and Wilson, 1998). This åkermanite–Na–åkermanite composition corresponds well to the typical igneous melilite of Velde and Yoder (1977), and contrasts with the unusual Fe- and Na-rich melilite from the evolved rocks, the melilite-bearing nephelinites of the more recent, mostly pyroclastic eruptions (Keller and Krafft, 1990, Wiedenmann, 2004). Dawson et al. (1989) explain some of the melilite compositions to be of metasomatic origin.

4.3.3. Nepheline

Nepheline has been described as rare microphenocrysts in the intergranular glass of the Armykon Hill and Lalarasi olivine melilitites and as abundant microphenocrysts in the groundmass of the Loolmurwak olivine–melilite nephelinite (Dawson et al., 1985). In contrast, nepheline is the most common constituent in the major rock types from Oldoinyo Lengai, the evolved nephelinites, phonolites, and ejected ijolitic blocks (Donaldson et al., 1987; Dawson et al., 1995b).

In the primitive olivine melilitite of Dorobo Cone, nepheline occurs as abundant euhedral microphenocrysts and rare phenocrysts. In the glassy groundmass of Armykon Hill, nepheline forms small euhedral crystals of up to 20 μm. Nepheline is also present in crystallised melt inclusions. Compared to other rock types the Dorobo nepheline contains very high K_2O (up to 11.6 wt.%). Na_2O is comparatively low, with 12.6–12.7 wt.% (Table 3 and Supplementary Table 9). With kalsilite contents between 35.9 and 37.4 mol%, the nepheline from Dorobo is the most potassic nepheline from any other African melilitite (Dawson et al., 1985). Nepheline from the crystallised melt inclusions has lower K_2O of 8.2 wt.%. This value is similar to an ideal stoichiometric $Na_3K(AlSiO_4)_4$ composition.

4.3.4. Clinopyroxene

Clinopyroxene is a ubiquitous mineral in all silicate rocks of Oldoinyo Lengai, but is rare in the olivine melilititic rocks of this discussion. Clinopyroxene occurs as scattered phenocrysts in Dorobo samples and in the groundmass of some samples. An exception is the samples of Oldoinyo Loolmurwak (Table 1). These ultrabasic melilite-bearing nephelinites have less modal melilite and a matrix dominated by clinopyroxene and magnetite. We follow Dawson et al. (1985) in distinguishing the latter as olivine–melilite nephelinites from the olivine melilitites in the centre of this study. Clinopyroxene occurs as euhedral prismatic crystals up to 600×300 μm in size. It commonly shows complex internal zoning with a round "green-core" (up to 100 μm in diameter) overgrown by diopsidic pyroxene (Fig. 3c). Green cores are highly heterogeneous and BSE images indicate variations in composition. The diopsidic outer zones are sometimes characterised by an oscillatory or sector zoning and also show irregular zonation in the form of patches and veins. The composition of the Dorobo clinopyroxene is variable ranging from aegirine–augite, Fe-rich diopside (almost hedenbergite) and diopside in green cores to diopside in the mantling zones (Table 3 and Supplementary Table 10; Fig. 4a). The brightest areas on BSE images (Fig. 3c) correspond to aegirine–augite and they contain highest FeO_{total} (up to 19.8 wt.%), Na_2O (up to 3.2 wt.%) and MnO (up to 0.7 wt.%) and lowest CaO (17.8 wt.%), MgO (5.8 wt.

%), Al_2O_3 (up to 0.5 wt.%) and TiO_2 (up to 0.2 wt.%). Compositions of the diopsidic outer zones are much less variable except for some variation in Al and Ti. Dark-gray zones on the BSE image (Fig. 3c) are characterised by lower Al_2O_3 (2.5–3.6 wt.%) and TiO_2 (1.8–2.4 wt.%) compared to light-gray areas with 4.3–4.9 wt.% Al_2O_3 and 2.7–3.4 wt.% TiO_2.

In Fig. 4, all published analyses of clinopyroxenes from different Oldoinyo Lengai rock types (in total 115 analyses) are plotted. Green-core clinopyroxenes of olivine melilitites have compositions similar to clinopyroxenes from older phonolites, nephelinites and some of the ijolitic plutonic blocks (Dawson et al., 1995b). In contrast, the mantling diopsides form a separate field with some similarity to clinopyroxenes from mica pyroxenites and olivine–mica ijolites.

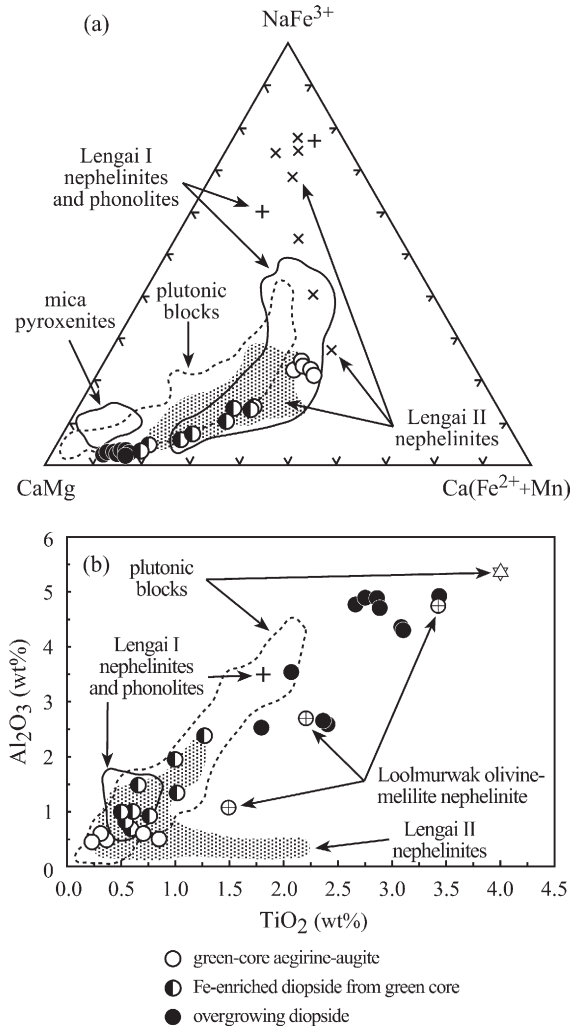

Fig. 4. (a) Clinopyroxene composition in the CaMg–$NaFe^{3+}$–Ca(Fe^{2+}+Mn) triangle and (b) clinopyroxene Al_2O_3–TiO_2 relationships. Data from mica pyroxenites, plutonic blocks, Lengai I nephelinites and phonolites and Lengai II nephelinites and from Dawson et al. (1985), Donaldson et al. (1987), Dawson and Smith (1992), Dawson et al. (1992, 1995b), Dawson (1998), and Dawson and Hill (1998).

The Dorobo olivine melilititic clinopyroxene has the greatest Al and Ti variation of all Oldoinyo Lengai rock types (Fig. 4b). Green-core compositions are similar to clinopyroxenes in nephelinites, phonolites and plutonic blocks, but mantling diopside forms a separate compositional field with highest Ti and Al compared to all other data. Only one analysis from a jacupirangite has higher Al and Ti.

4.3.5. Garnet

Garnet is a very rare mineral in olivine melilitites. The garnet is round dark-brown, 500 μm in diameter and partly replaced by melilite. The garnet is classified as schorlomite (Howie and Woolley, 1968) with TiO_2 contents between 17.7 and 20.3 wt.% (Table 3 and Supplementary Table 11). This is the highest Ti content reported from nephelinites and ijolites of Oldoinyo Lengai (Donaldson et al., 1987; Dawson et al., 1995b; Dawson, 1998; Dawson and Hill, 1998). The analyses show low MgO (0.7–1.3 wt.%), Al_2O_3 (0.3–0.6 wt.%) and MnO (0.2–0.4 wt.%), and contain between 0.2 and 0.4 wt.% Na_2O, a feature common for garnets from other Lengai rocks (Dawson et al., 1995a,b). Zr contents (0.6 to 1.2 wt.% ZrO_2) are similar to schorlomite in nephelinites and ijolites. An unusual feature of the analyzed schorlomite is the relatively high V_2O_3 of 0.3 to 0.9 wt.%.

Although melanitic–schorlomitic garnets are exceedingly rare in olivine melilitites (but rather common in the evolved phonolites and nephelinites), it appears unlikely that garnet is a xenocryst, because all published data for garnets from other rock types are distinct. This is particularly obvious in their much lower Ti contents.

4.3.6. Spinel

Spinel is common in all olivine melilitites from Oldoinyo Lengai (Table 3 and Supplementary Table 12). In the Armykon Hill and Dorobo Cone samples, spinels occur as (1) euhedral crystals 50–100 μm in size as inclusions in olivine and (2) relatively large euhedral groundmass crystals of 100–250 μm in size. They form two distinct populations that range in composition from Mg-, Al- and Ti-rich chromium spinel as inclusions in olivine that evolve to Mg-rich to titaniferous magnetite in the groundmass (Dawson et al., 1985; Fig. 5). Tiny euhedral microcrysts (5–20 μm) in the groundmass matrix occur as variety (3) which are compositionally similar to the intermediate zones of "phenocrysts" of the

second variety. This spinel composition is characterised by 11.7–12.3 wt.% TiO_2, 6.3–7.7 wt.% Cr_2O_3, 7.0–7.6 wt.% MgO and 3.1–3.4 wt.% Al_2O_3.

In addition to inclusions in olivine (Dawson et al., 1985), Cr-spinel also occurs as core in many groundmass spinels. The Cr-spinel contains up to 38.2 wt.% Cr_2O_3, 12.0 wt.% Al_2O_3, 9.6 wt.% MgO and 4.0 wt.% TiO_2. Spinel evolves from cores with high Cr/(Cr+Al) ratios of 0.68–0.77 and low Ti/(Ti+Cr+Al) and Fe^{2+}/(Fe^{2+}+Mg) ratios (0.06–0.19 and 0.56–0.64 respectively) through inner rim compositions with Cr/(Cr+Al)=0.55–0.74, Ti/(Ti+Cr+Al)=0.18–0.56 and Fe^{2+}/(Fe^{2+}+Mg)=0.66–0.75, to low Cr/(Cr+Al) of 0–0.27, high Ti/(Ti+Cr+Al)=0.76–0.87 and Fe^{2+}/(Fe^{2+}+Mg)=0.75–0.81 compositions in the outermost rims. BSE images show gradational changes in spinel compositions, and no resorption features are evident.

4.3.7. Perovskite

Perovskite is a major phase in the mineralogy of the olivine melilitites. It occurs generally as euhedral, round or oval crystals, up to 100–400 μm in size. Large euhedral perovskites with the appearance of phenocrysts (up to 5 mm) are present in olivine melilitites from Armykon Hill (OL 12).

The olivine–melilite nephelinites from Loolmurwak cone differ from the olivine melilitites by their lower contents of perovskite; in these, perovskite is restricted to microcrystals in a magnetite–clinopyroxene-dominated groundmass.

BSE images reveal a complex internal structure of the perovskite crystals of different morphological types. Euhedral crystals commonly show bright euhedral homogeneous cores (high average atomic number) and gray-toned rims (lower average atomic number). Sometimes, thin (1–5 μm) bright areas are observed within rim zones that are parallel to crystal shapes (oscillatory-like zoning). Round or oval crystals of perovskite are characterised by a more complex pattern in their internal structure (Fig. 3d). They normally have round or oval-shaped cores, that are either compositionally heterogeneous or homogeneous, and rims of alternating 1 to 10 μm thick zones. Perovskite phenocrysts from OL 12 (Armykon) are homogeneous on BSE images. X-ray element distribution maps show a slight depletion in Nb towards the rims and an erratic Na distribution.

Electron microprobe analyses (Table 3 and Supplementary Table 13) show that the difference in contrast on BSE images of the perovskite is mainly due to variations in REE contents. Euhedral crystals contain 1.63 to 1.89 wt.% REE_2O_3 in the core and significantly less in the rim (0.57–1.24 wt.% REE_2O_3). Other elements such as Fe, Nb, Na and Sr do now show variations between core and rim. Contents of Th, U, Pb, Ta and Zr are below 0.2 wt.% of their oxides. The perovskite from Armykon Hill and Dorobo Cone (Supplementary Table 13) and those from Lalarasi and Armykon Hill melilitites of Dawson et al. (1985) are distinct from perovskite compositions from other Lengai rock types. Perovskite in nephelinites and in plutonic blocks of jacupirangite and ijolite shows enrichment in REE_2O_3 (up to 7.0 wt.%), Nb_2O_5 (up to 1.5 wt.%), Na_2O (up to 1.0 wt.%) and SrO (up to 0.5 wt.%) compared to perovskite in melilitites (Dawson et al., 1985, 1995b; Dawson, 1998). Perovskite in the combeite–lamprophyllite nephelinite of Dawson and Hill (1998) is distinctly enriched containing 4.9–5.7 wt.

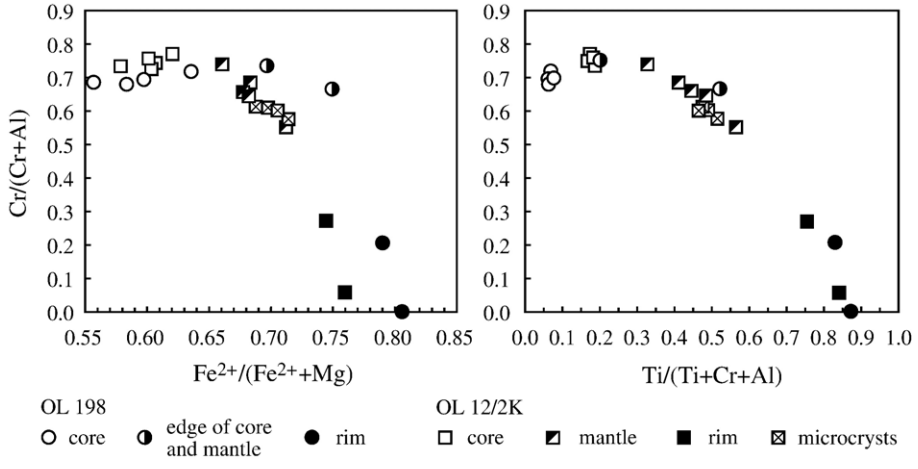

Fig. 5. Cr–Fe–Ti–Mg relationships in spinel group minerals.

% Na_2O, 8.4–9.0 wt.% Nb_2O_5, 9.2–9.5 wt.% SrO and 12.6–16.3 wt.% REE_2O_3.

Among the REE, only the lighter elements have been detected by electron microprobe. Heavy REE and Y are present in amounts of <0.1 wt.%. The chondrite-normalized REE patterns of perovskite from various samples are different. Core and rim of perovskite from Dorobo olivine melilitite show a similar (near parallel) pattern with an average La/Ce_{CN} ratio (CN = chondrite normalized) of 0.97 and 1.02 for core and rim, respectively. The perovskite from Armykon Hill (OL 12) exhibits a more complex REE pattern. Cores show depletion in La relative to Ce with an average La/Ce_{CN} of 0.78. The La/Ce_{CN} ratio increases towards the outer part of the cores (average La/Ce_{CN} = 1.13). Similar patterns are observed in the rims of the perovskite with La/Ce_{CN} of 1.07. Large phenocrystic perovskite is characterised by a maximum enrichment in La compared to all other data with an average La/Ce_{CN} ratio of 1.18.

4.3.8. Crystallised melt inclusions

A few melt inclusions (up to 70 × 40 μm) have been found in groundmass magnetite in sample OL 198. They are subhedral to round and contain several mineral phases. Electron microprobe data suggest that the minerals are olivine (Fo = 81, NiO = 0.04 wt.%), melilite (MgO = 8.4 wt.%, FeO = 4.5 wt.%), nepheline (K_2O = 8.2 wt.%) and apatite. The compositions of olivine and melilite suggest that the minerals have crystallised from a slightly "evolved" melt, after crystallisation of phenocrystic olivine and melilite.

4.3.9. Sr-bearing baryte and calcite

Baryte is a rare mineral occurring in the groundmass as anhedral crystals up to 20 μm in size. A few veins of calcite (20–30 μm in thickness) have been observed in sample OL 198. A small Sr peak is visible in the electron microprobe EDS.

4.4. Chemical composition of olivine melilitites

4.4.1. Major element geochemistry

Chemical data for olivine melilitites at Oldoinyo Lengai and from the nearby tuff cones (DC, AH, SL) define two groups (1) with high magnesian members (Mg# 70, high Ni and Cr contents) which are likely candidates for primary mantle melts (Fig. 6a), and (2) more fractionated compositions with Mg# <60 as from Armykon Hill and Lalarasi (Dawson et al., 1985). Table 1 reports major and trace element data for the primitive olivine melilitites (DC, SL) and for the more evolved types (AH, partly SL and additional data from the melilititic pyroclastics of Kirurum parasitic crater). A common chemical feature is the general peralkaline trend with (Na + K)/Al > 1. Dawson (1998) noted that available melilitite compositions from Armykon Hill and Lalarasi (Dawson et al., 1985) have evolved Mg#. Therefore, the olivine–melilite nephelinite of Oldoinyo Loolmurwak was taken as the best approximation for a primary composition of the area (Peterson and Kjarsgaard, 1995; Dawson, 1998). The peralkalinity index for the olivine–melilite nephelinites of Oldoinyo Loolmurwak is constantly <1 as shown by the analyzed samples OL 141, 199, 342 from different parts of Oldoinyo Loolmurwak (Table 1). Thus, olivine–melilite nephelinite of Oldoinyo Loolmurwak differs from the primitive Oldoinyo Lengai olivine melilitites. There exists also an apparent age difference. K/Ar ages from 0.53 to 0.14 m.y. have been obtained on micas

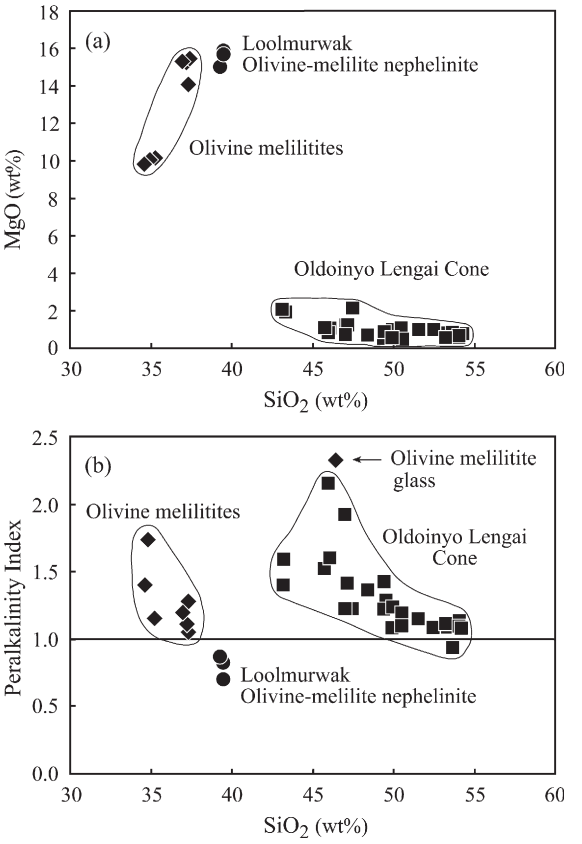

Fig. 6. (a) MgO vs. SiO_2 relationship in evolved silicate lavas of the Oldoinyo Lengai cone (nephelinites, phonolites) and olivine melilitites and (b) peralkalinity Index (K + Na)/Al vs. SiO_2 relationship in silicate lavas (nephelinites, phonolites) and olivine melilitites. Nephelinites and phonolites of OL Cone—data from Donaldson et al. (1987) and Klaudius and Keller (2006-this issue), olivine melilitites—this study.

from the Loolmurwak crater (McIntyre et al., 1974), contrasting with the sub-Recent age of Dorobo, Lalarasi and probably Armykon olivine melilitites.

With the most primitive compositions at Dorobo and Lalarasi thought to represent primary mantle-derived melts, the olivine melilitites at Lengai show a peralkaline composition from the beginning (Fig. 6b). This points to particular conditions in the mantle region of partial melting underneath Oldoinyo Lengai. Peralkalinity became more pronounced with fractionation as shown by the more evolved Lalarasi flow and the Armykon Hill lavas, and in particular by the matrix glass composition of this latter olivine melilitite with (Na+K)/Al=2.33 (Table 1). Olivine fractionation is the dominant process in the early steps of differentiating primitive olivine melilitites. As clinopyroxene is not an important low-pressure phenocryst phase in the olivine melilitite, spinel and melilite fractionation is suggested to contribute to the increasing peralkalinity.

In more general terms, the olivine melilitites of this study compare with melilitites from other rift areas (Brey, 1978; Keller et al., 1990; Wilson et al., 1995; Hegner et al., 1995; Dunworth and Wilson, 1998) in terms of their low SiO_2, low Al_2O_3, normative larnite content and relatively high CaO and incompatible element concentrations. In addition to the peralkaline trend, the primitive olivine melilitites at Oldoinyo Lengai are characterised by enhanced K contents as expressed in K_2O/Na_2O ratios of >0.5. All olivine melilitites from the Lengai-Lake Natron area are further distinguished by their high TiO_2 (4.2–5.8 wt.%). These unusually high TiO_2 contents have already been observed in the data set of Dawson et al. (1985) which comprises the evolved olivine melilitites with Mg# ≤60. Table 1 shows TiO_2 contents of 4–4.5 wt.% already in the primitive compositions and an increase up to 5.8 wt.% with early olivine fractionation. With magnetite and perovskite removal during further fractionation, TiO_2 decreases again to 4.3 wt.% in the Kirurum melilitite, and to 3 wt.% in the Armykon glass composition with its Mg# of 39 (Table 1). The Kirurum melilitite is the most fractionated of the analyzed olivine melilitites with an Mg# of 51 and Ni down to 12 ppm (Table 1). Here, the trend of increasing TiO_2 that is observed in the step from high-Mg compositions of Dorobo to Armykon Hill is reversed and Ti decreases presumably due to perovskite and Ti-magnetite fractionation.

4.4.2. Trace element chemistry

A set of the petrologically important trace elements is reported in Tables 1 and 2. These show the range of compatible and incompatible element contents for the primitive olivine melilitites, and the behaviour during fractionation from Mg# 70 (OL 198B) to the moderately evolved compositions with Mg# down to 59 (OL 12). This fractionation step is dominantly olivine-controlled. The LREE, if considered ideally incompatible for this step, indicate the separation of about 30 vol.% crystals. Similar trends show other incompatible elements, in particular Nb, Y, Zr, Hf, Th, Ta. In the primitive mantle (PM)-normalized consideration of incompatible element variation (Fig. 7), and in the chondrite-normalized plot of the REE (Fig. 8), the degrees of enrichment of the primitive olivine melilitites and of the evolved compositions are shown. LIL elements are 100–200 times PM and the LREE 300–500 times chondritic. La/Yb_{CN} and La/Sm_{CN} ratios are 38–46 and 3.8–4.6, respectively, and define the LREE/HREE enrichment.

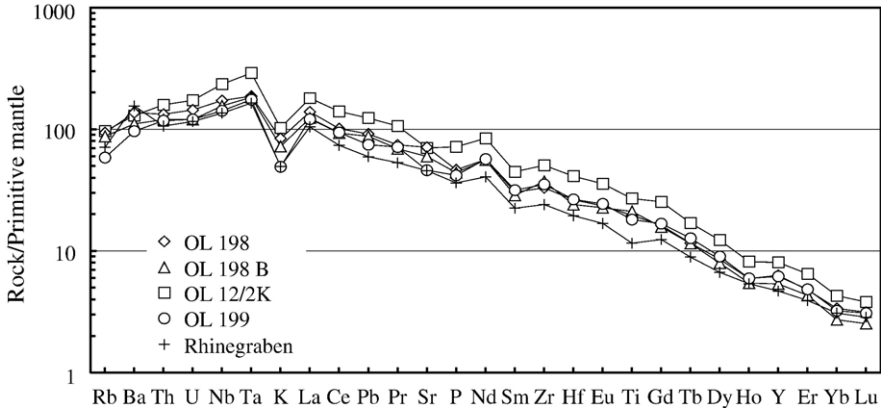

Fig. 7. Primitive mantle normalized incompatible trace element abundances in olivine melilitites. Rhinegraben data from Keller et al. (1990). Normalizing values from McDonough and Sun (1995).

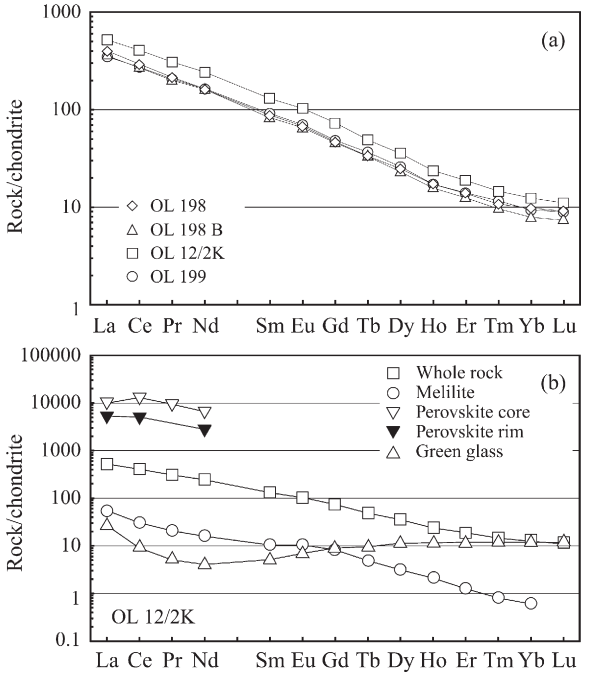

Fig. 8. (a) Chondrite-normalized REE diagram for olivine melilitites and (b) REE abundances for melilitite green glass, compared to bulk rock, melilite and perovskite. Normalizing values from McDonough and Sun (1995).

The general pattern of the incompatible element variation is very similar to olivine melilitites from elsewhere. This is shown with a representative olivine melilitite from the Rhinegraben for comparison (Fig. 7). The similarity includes the negative K anomaly (relative to adjacent Ta and La in the normalized plot) which may point to residual phlogopite or amphibole in the regime of low-percentage melting (Wilson and Downes, 1991). Le Roex et al. (2001) argued that the basaltic rocks of the southern Kenya rift with a negative K anomaly formed by partial melting of an amphibole-bearing lherzolite mantle.

The enrichment of LIL and REE elements against primitive mantle averages (Sun and McDonough, 1989; McDonough and Sun, 1995) underlines very low-percentage melting, as commonly accepted for olivine melilitites (Brey, 1978; Keller et al., 1990; Hegner et al., 1995; Dunworth and Wilson, 1998). Inter-element ratios have been discussed for the Kenyan sector of the East African rift in terms of possible plume–lithosphere interaction (e.g. Macdonald et al., 2001). Zr/Hf ratios range from 45 to 56, slightly higher than the rather constant OIB value of 36 (Sun and McDonough, 1989). Zr/Nb is 3–4, Nb/Ta and Hf/Ta average to 15 and 1.1, respectively (using the ICP-MS data in Table 1). Both ratios are lower than characteristic OIB values. Ce/Pb ratios vary only slightly from 27 to 31 and are similar to a constant OIB value of 25±5 (Sun and McDonough, 1989). Ce/Pb as well as Ba/U are sensitive parameters for crustal contamination but fall within the range of mantle derived melts. The Ce/Y ratio of 6–7 for the primitive olivine melilitites is consistent with a garnet controlled source.

An estimation for the melting percentage is derived from incompatible trace inter-element modelling as obtained by Macdonald et al. (2001) for primitive mafic rocks of the East African Rift. Fig. 9 uses the Zr/Nb and Ce/Y variation, following the modelling of Hardarson and Fitton (1991). For the primitive olivine melilitites, this points to very low melting degrees in the order of only a few % or less, and reinforces the presence of garnet in the source. Melting for primary olivine melilitites is thought to occur in the depth range of about 100 km according to experimental results (Brey, 1978). In contrast, Furman et al. (2004) derive a rather shallow depth of melting for basic melts in the northern sector of the Kenya rift segment.

The vitrophyric nature of OL 12/2K from Armykon Hill with its distinct green glass matrix (Fig. 2) allow an estimation of the residual melt composition with a high degree of crystallisation of the olivine melilitite. Tables 1 and 2 report LA ICP-MS trace element data for this glass. Due to melilite, perovskite and apatite crystallisation, almost none of the analyzed trace elements remains incompatible, with the possible exception of Zr and Hf. The extreme depletion of the light and middle REE (Fig. 8b) is explained by the high degree of

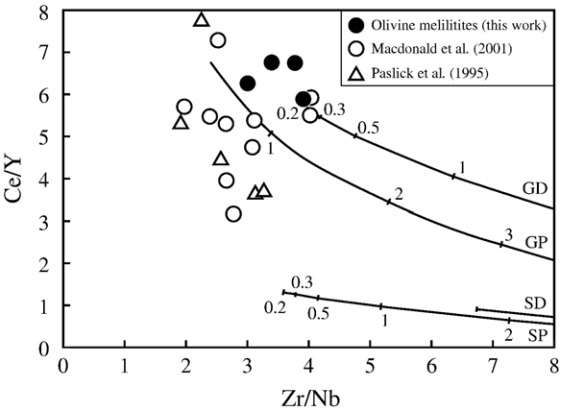

Fig. 9. Partial melting relations for mafic rocks of the East African Rift in Ce/Y vs. Zr/Nb space, adopted from Macdonald et al. (2001). Lines with numbers (for melt percentages) are non-modal melting curves from Hardarson and Fitton (1991). Mantle compositions are: GP, GD primitive resp. depleted garnet lherzolite; SP, SD primitive resp. depleted spinel lherzolite.

Table 4
Sr–Nd–Pb isotope data from olivine melilitites

Sample	Locality	Occurrence	$^{87}Sr/^{86}Sr$	$^{143}Nd/^{144}Nd$	$^{206}Pb/^{204}Pb$	$^{207}Pb/^{204}Pb$	$^{208}Pb/^{204}Pb$
OL 198	Dorobo Cone	lava block	0.703788	0.512767	19.861	15.691	39.765
OL 199	Loolmurwak	lava block	0.703689	0.512759	20.047	15.706	39.756
OL 12/99	Armykon Hill	lava block	0.703641	0.512773	19.932	15.669	39.739
OL 12/2K	Armykon Hill	lava flow	0.703638	0.512773			

perovskite crystallisation with its La, Ce, etc. contents of 10,000 times chondritic (Table 2). It is inferred from this observation, that any possible fractionation path from primitive olivine melilitites towards the extremely evolved and incompatible element-enriched peralkaline wollastonite–combeite nephelinites of Lengai (Keller and Spettel, 1995; Dawson, 1998; Klaudius and Keller, 2006-this issue) must be dependent on separation of the residual melt before extensive perovskite crystallisation.

4.4.3. Radiogenic isotope systematics: Sr, Nd, and Pb isotopes

There is a considerable body of isotope data available for northern Tanzania and the adjacent south Kenya rift sector in general (Cohen et al., 1984; Paslick et al., 1995; Kalt et al., 1997; Le Roex et al., 2001), and also focused on Oldoinyo Lengai itself (Bell and Dawson, 1995; Bell and Simonetti, 1996; Bell and Tilton, 2001), but no isotopic data for the olivine melilitites of this study were available. Sr, Nd and Pb isotope data are presented in Table 4.

The Sr and Nd isotopic composition of Oldoinyo Lengai lavas is characterised by an extremely large variation (Bell and Dawson, 1995). This is shown in the Nd–Sr isotope systematics of Fig. 10 where the Lengai rocks plot along the EACL (East African Carbonatite Line; Bell and Blenkinsop, 1987) that connects the HIMU and EM I compositions. Nephelinites form two distinct groups (Bell and Dawson, 1995; Bell and Simonetti, 1996; Dawson, 1998) where Group I represents the CWN of the young Lengai II. Recent natrocarbonatites overlap with the field of recent combeite–wollastonite nephelinites of Group I (Keller and Krafft, 1990; Bell and Dawson, 1995). Natrocarbonatite and CWN silicate lavas can be considered isotopically identical. The isotopically more enriched Group II nephelinites is stratigraphically less well constrained, but it appears that Group II is older than the CWN of recent Lengai II. Phonolites of the southern cone of Oldoinyo Lengai straddle the gap between the two groups. Bell and Dawson (1995) and Kramm and Sindern (1998) have further included plutonic cumulates and fenites in this picture.

Data for the olivine melilitites presented here (Table 4, Fig. 10) form again a distinct and clearly separated group in their Sr–Nd isotope systematics. The observed heterogeneity of sources for the lavas of Oldoinyo Lengai (Bell and Dawson, 1995) is further underlined by the isotope data of this study. With an average $^{87}Sr/^{86}Sr$ of 0.703688 and $^{143}Nd/^{144}Nd$ of 0.512767 the olivine melilitites are significantly more depleted as compared to the two nephelinite groups and the straddling phonolite field of Oldoinyo Lengai (Fig. 10).

When the Lengai variation is explained as a two-mantle-component mixing (Bell and Dawson, 1995; Bell and Tilton, 2001), then the olivine melilitites are the lavas closest to the assumed HIMU end member. It is worth noting with reference to Bell and Dawson (1995) that the olivine melilitite data approach the composition of the even more depleted mantle xenoliths from Eledoi and Pello tuff cones about 10 km east of Oldoinyo Lengai (Dawson and Smith, 1988; Bell and Dawson, 1995). Mantle xenoliths from the tuff cones may represent the isotopic composition of the mantle source of Oldoinyo Lengai olivine melilitites, but are likely to have been metasomatised to some extent.

Pb isotopes of the evolved silicate rocks from Oldoinyo Lengai and of the natrocarbonatites have been discussed by Bell and Simonetti (1996). It was shown that Oldoinyo Lengai samples have very low radiogenic Pb ratios. Bell (1998) has added Pb isotope data for Shombole that define a distinct, more radiogenic field in all lead isotope plots compared to Oldoinyo Lengai. Paslick et al. (1995) reported Pb isotopes for Kerimasi carbonatites. It is interesting to note that both carbonatite complexes, Shombole to the north and Kerimasi to the south, have higher Pb isotope ratios than the Oldoinyo Lengai phonolite–nephelinite–natrocarbonatite group. In Table 4 and Fig. 11, Pb isotope data for the olivine melilitite group and for the olivine melilite nephelinite of Loolmurwak are presented. The correlation within the Sr–Nd–Pb systems is shown in Fig. 12. Average ratios for the Pb isotopes are $^{208}Pb/^{204}Pb = 39.784$, $^{207}Pb/^{204}Pb = 15.688$ and $^{206}Pb/^{204}Pb = 19.947$ (Table 4).

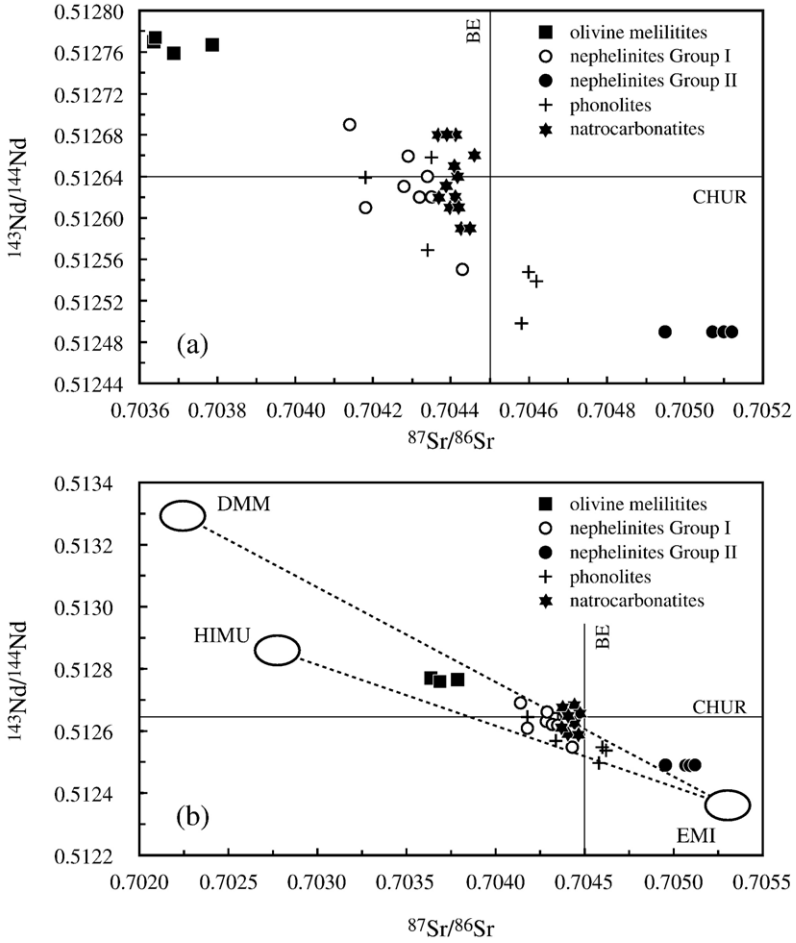

Fig. 10. Sr and Nd isotope variation (a) in Oldoinyo Lengai lavas and olivine melilitites and (b) Sr and Nd isotope data relating different isotopic groups at Oldoinyo Lengai to mantle end-member components (b). Data sources: olivine melilitites—this study; nephelinites Group I and II, phonolites and natrocarbonatites from Bell and Blenkinsop (1987), Keller and Krafft (1990), Bell and Peterson (1991), Bell and Dawson (1995), Bell and Simonetti (1996), Kramm and Sindern (1998) and Bell and Tilton (2001). Mantle component compositions as used in Bell and Tilton (2001).

Pb isotopes of the rift area are interpreted by Bell (1998), and Bell and Tilton (2001) to confirm the mixing of HIMU and EM I end members. At Lengai, Pb isotope plots show the olivine melilitites separated, but also distinct fields for phonolites and for nephelinites. The two separate groups of nephelinites (Group I and Group II nephelinites) of Dawson (1998) are distinguished by different Sr and Nd isotope ratios, but not distinct in terms of their Pb isotopes.

5. Discussion and conclusions

The data presented in this paper provide evidence for the presence of primitive high-Mg lavas at Oldoinyo Lengai. Olivine melilitites in the immediate vicinity of Oldoinyo Lengai, that are closely related in time and in space with the recent Oldoinyo Lengai evolution, are unequivocal candidates for primary magma compositions. In particular, the Dorobo Cone is a young parasitic vent of Oldoinyo Lengai in close volcanological connection with the main cone. Similar high-Mg olivine melilitites have been identified at the more excentric Sinja-Lalarasi Cone. No other high-Mg compositions exist at Oldoinyo Lengai. Phase petrology, high MgO ($\geq$15 wt.%), and related compatible trace elements (Ni, Cr), combined with the enriched incompatible element compositions suggest a low-percentage melting regime in the asthenospheric mantle. Dawson (1998) proposed carbonated olivine nephelinite (the olivine–melilite nephelinite of the Loolmurwak group) as the model primary composition for the Lengai evolution, as primary olivine melilitite had not been detected before. The new data provide a distinction between these melilite-bearing olivine

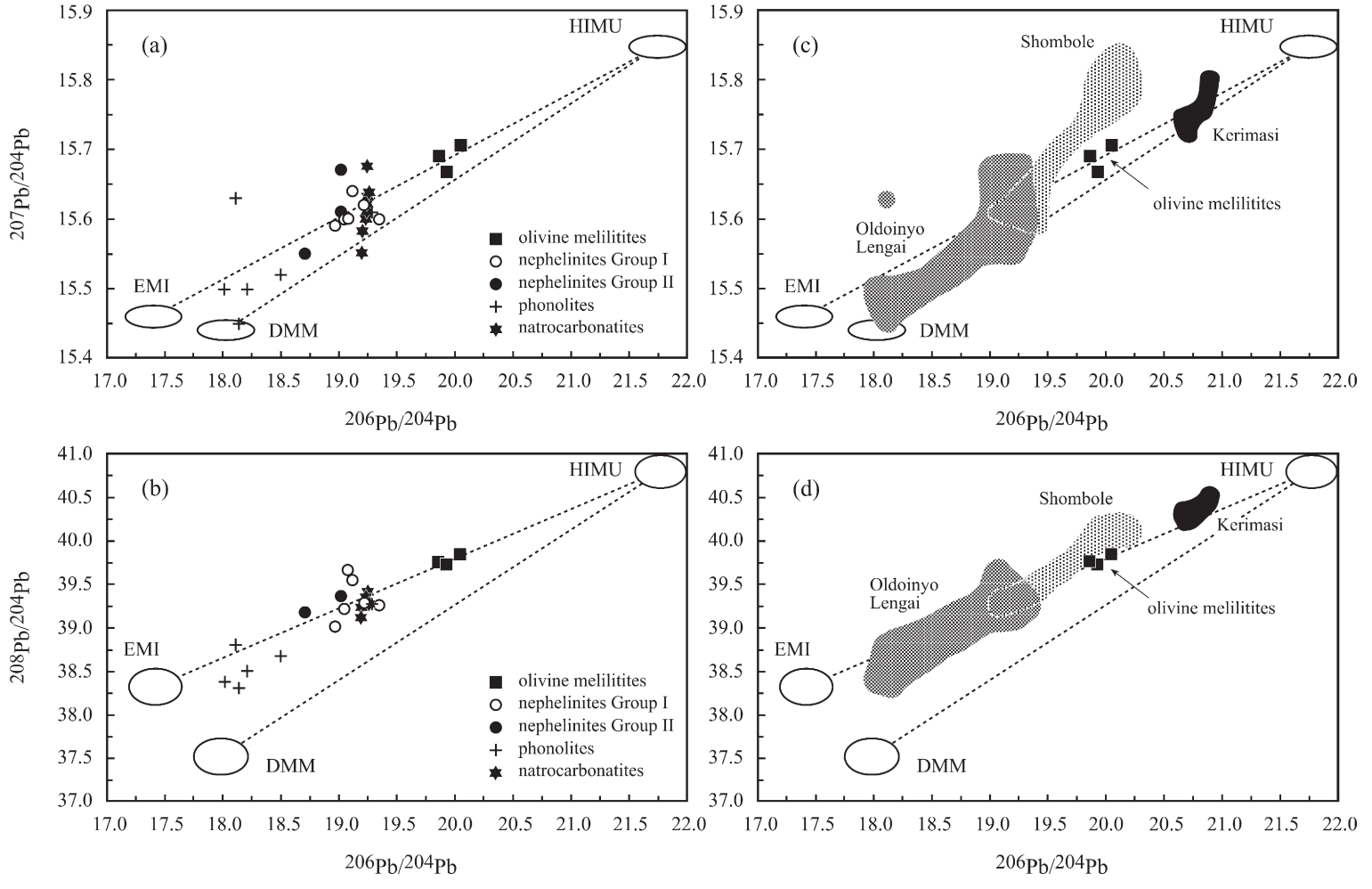

Fig. 11. Pb–Pb isotope variations at Oldoinyo Lengai: (a) $^{207}Pb/^{204}Pb$–$^{206}Pb/^{204}Pb$ correlation diagram and (b) $^{208}Pb/^{204}Pb$–$^{206}Pb/^{204}Pb$ correlation diagram and Pb–Pb isotopic systematics of olivine melilitites compared to other Oldoinyo Lengai silicate lavas; Shombole and Kerimasi: (c) $^{207}Pb/^{204}$–Pb–$^{206}Pb/^{204}Pb$ correlation diagram and (d) $^{208}Pb/^{204}Pb$–$^{206}Pb/^{204}Pb$ correlation diagram. Data sources as in Fig. 10 and Paslick et al. (1995). Mantle component compositions as used in Bell and Tilton (2001).

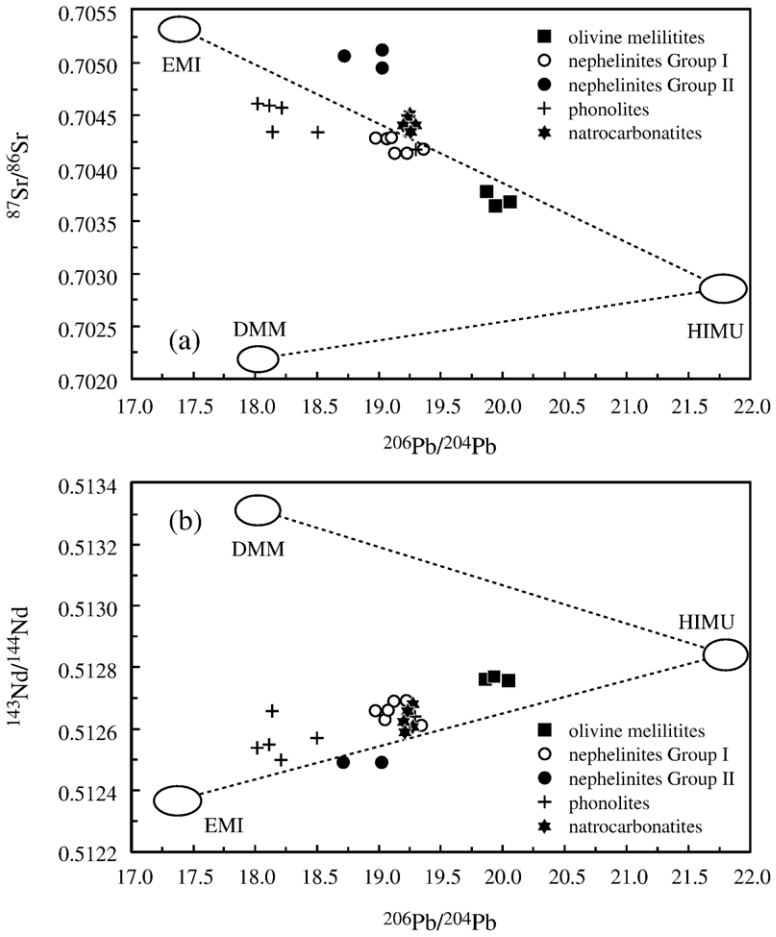

Fig. 12. Sr and Nd vs. Pb isotopic compositions for Oldoinyo Lengai rocks. $^{87}Sr/^{86}Sr$ vs. $^{206}Pb/^{204}Pb$ (a) and $^{143}Nd/^{144}Nd$ vs. $^{206}Pb/^{204}Pb$ (b). Data sources as in Fig. 10. Mantle component compositions as used in Bell and Tilton (2001).

nephelinites of the Loolmurwak group and olivine melilitite (s.s.) as primary composition in the rift of the Oldoinyo Lengai vicinity.

The peralkaline character of all Oldoinyo Lengai lavas, particularly pronounced in the combeite–wollastonite nephelinites (CWN) of Recent Lengai, is already recognised in these primary or near-primary melts. It is shown that all analyzed olivine melilitites, even the most primitive ones, are peralkaline with (Na+K)/Al>1.0. More evolved olivine melilitites with Mg#<60 allow the first steps of a fractionation line in its major and trace element expression to be followed.

Peterson and Kjarsgaard (1995) and Kjarsgaard et al. (1995) start the production of highly peralkaline nephelinites with olivine melilitite, whereas the less alkaline olivine nephelinites (like the Loolmorwak compositions) would be the primary compositions for the older and less alkaline phonolites and nephelinites of Lengai I. Modelled by Peterson and Kjarsgaard (1995) in the system Ne–Ab–Ln–Fo, melts corresponding to olivine melilitite will fractionate towards the highly peralkaline nephelinites with MgO <2.0 wt.% and Mg# <30. Nevertheless, a large compositional gap (still) separates the olivine melilitites and olivine-poorer melilitites from the highly evolved phonolites and peralkaline nephelinites with MgO contents <2 wt.%, that form the bulk of the Lengai volcano. Thus, the remaining problem is the lack of any intermediate compositions, in addition to the isotopic heterogeneity.

Oldoinyo Lengai is characterised by an extreme spread in isotopic ratios (Bell and Dawson, 1995). However, the reported Nd, Sr and Pb isotopic data for olivine melilitites from Dorobo Cone and Armykon Hill, and for olivine–melilite nephelinites from the Loolmurwak group (Table 4) show a narrow range with

averages given above. The field for the olivine melilitites in the isotope diagrams is always distinctly separated from the fields that include combeite–wollastonite nephelinites and natrocarbonatites. The Sr, Nd, and Pb isotope data for the olivine melilitites represent the most depleted compositions in the Sr–Nd isotope diagram and the most radiogenic Pb isotope relationships for Oldoinyo Lengai. The new data are closest to a supposed HIMU end member of the Lengai evolution, which is explained as a mixing line between HIMU and EM1-like mantle components.

If the high-Mg group of olivine melilitites is considered the primary composition for the Lengai evolution by fractionation, the mixing of these HIMU type melts with an isotopically different component has to be invoked. While primitive olivine melilitite reached the surface uncontaminated, residence and fractionation in the lithosphere, identified as enriched mantle (EM I), has occurred between the olivine melilitite melting and the eruption of enriched nephelinites of the CWN compositions (and isotopically identical natrocarbonatites; Keller and Krafft, 1990). The differences in isotopic compositions between primary melts–the olivine melilitites of this paper–and the evolved CWN nephelinite and associated, isotopically identical natrocarbonatite require complex models of open-system source mixing during or before an assumed evolution by fractionation.

Acknowledgements

Assistance in the field was provided by Jurgis Klaudius from IMPG Freiburg, the Dorobo organisation Arusha, Chris Weber of VEI, and Burra Ami Gadiye from Engare Sero. We are grateful to Terry Williams and Teresa Jeffries (The Natural History Museum, London) for access to analytical facilities of NHM and assistance with microprobe and LA ICP-MS analyses. Keith Bell (Carleton University, Ottawa) kindly provided the Pb isotope measurements. Sr and Nd isotopes were performed by M. Satir, Tübingen. ICP-MS data for trace elements were obtained through J. Morel of CRPG-CNRS Nancy, France. Rodney Grapes is thanked for polishing the English of an early version of the manuscript. This paper stems from research project KE 136/40 funded generously by Deutsche Forschungsgemeinschaft (DFG). Anatoly N. Zaitsev acknowledges an Alexander von Humboldt Fellowship.

We enjoyed the careful reviews by Barry Dawson and Adrian Jones and the patient editorial guidance of Gregor Markl.

Appendix A. Supplementary data

Supplementary data associated with this article can be found, in the online version, at doi:10.1016/j.lithos.2006.03.014.

References

Bell, K., 1998. Radiogenic isotope constrains on relationships between carbonatites and associated silicate rocks—a brief review. J. Petrol. 39, 1987–1997.

Bell, K., Blenkinsop, J., 1987. Nd and Sr isotopic composition of East African carbonatites: implications for mantle heterogeneity. Geology 15, 99–102.

Bell, K., Dawson, J.B., 1995. Nd and Sr isotope systematics of the active carbonatite volcano, Oldoinyo Lengai. In: Bell, K., Keller, J. (Eds.), Carbonatite Volcanism: Oldoinyo Lengai and the Petrogenesis of Natrocarbonatites. IAVCEI Proceedings in Volcanology, vol. 4. Springer Verlag, Berlin, pp. 113–123.

Bell, K., Peterson, T., 1991. Nd and Sr isotope systematics of Shombole volcano, East Africa, and the links between nephelinites, phonolites, and carbonatites. Geology 19, 582–585.

Bell, K., Simonetti, A., 1996. Carbonatite magmatism and plume activity: implication from the Nd, Pb and Sr isotope systematics of Oldoinyo Lengai. J. Petrol. 37, 1321–1339.

Bell, K., Tilton, G.R., 2001. Nd, Pb and Sr isotopic compositions of east African carbonatites: evidence for mantle mixing and plume inhomogeneity. J. Petrol. 42, 1927–1945.

Brey, G., 1978. Origin of olivine melilitites—chemical and experimental constraints. J. Volcanol. Geotherm. Res. 3, 61–88.

Church, A.A., Jones, A.P., 1995. Silicate–carbonate immiscibility at Oldoinyo Lengai. J. Petrol. 36, 869–889.

Cohen, R.S., O'Nions, R.K., Dawson, J.B., 1984. Isotope geochemistry of xenoliths from East Africa: implications for the development of mantle reservoirs and their interaction. Earth Planet. Sci. Lett. 68, 209–220.

Dawson, J.B., 1962. The geology of Oldoinyo Lengai. Bull. Volcanol. 24, 348–387.

Dawson, J.B., 1989. Sodium carbonate lavas from Oldoinyo Lengai, Tanzania: implications for carbonatite complex genesis. In: Bell, K. (Ed.), Carbonatites—Genesis and Evolution. Unwin Hyman, London, pp. 255–277.

Dawson, J.B., 1998. Peralkaline nephelinite–natrocarbonatite relationships at Oldoinyo Lengai, Tanzania. J. Petrol. 39, 2077–2095.

Dawson, J.B., Hill, P.G., 1998. Mineral chemistry of a peralkaline combeite–lamprophyllite nephelinite from Oldoino Lengai, Tanzania. Mineral. Mag. 62, 179–196.

Dawson, J.B., Powell, D.G., 1969. The Natron-Engaruka explosion crater area, Northern Tanzania. Bull. Volcanol. 33, 761–817.

Dawson, J.B., Smith, J.V., 1988. Metasomatized and veined upper mantle xenoliths from Pello Hill, Tanzania: evidence for anomalously-light mantle beneath the Tanzanian sector of the East African Rift Valley. Contrib. Mineral. Petrol. 100, 510–527.

Dawson, J.B., Smith, J.V., 1992. Olivine–mica pyroxenite xenoliths from northern Tanzania, metasomatic products of upper-mantle peridotite. J. Volcanol. Geotherm. Res. 50, 131–142.

Dawson, J.B., Bowden, P., Clark, G.C., 1968. Activity of the carbonatite volcano Oldoinyo Lengai, 1966. Geol. Rundsch. 57, 865–879.

Dawson, J.B., Smith, J.V., Jones, A.P., 1985. A comparative study of bulk rock and mineral chemistry of olivine melilitites and associated rocks from East and South Africa. Neues Jahrb. Mineral. Abh. 152, 143–175.

Dawson, J.B., Smith, J.V., Steele, I.M., 1989. Combeite ($Na_{2.33}Ca_{1.74}$-$others_{0.12}$)Si_3O_9 from Oldoinyo Lengai, Tanzania. J. Geol. 97, 365–372.

Dawson, J.B., Smith, J.V., Steele, I.M., 1992. 1966 ash eruption of the carbonatite volcano Oldoinyo Lengai: mineralogy of lapilli and mixing of silicate and carbonate magmas. Mineral. Mag. 56, 1–16.

Dawson, J.B, Keller, J., Nyamweru, C., 1995a. Historic and recent eruptive activity of Oldoinyo Lengai. In: Bell, K., Keller, J. (Eds.), Carbonatite Volcanism: Oldoinyo Lengai and the Petrogenesis of Natrocarbonatites. IAVCEI Proceedings in Volcanology, vol. 4. Springer Verlag, Berlin, pp. 4–22.

Dawson, J.B., Smith, J.V., Steele, I.M., 1995b. Petrology and mineral chemistry of plutonic igneous xenoliths from the carbonatite volcano, Oldoinyo Lengai, Tanzania. J. Petrol. 36, 797–826.

Dawson, J.B., Pyle, D.M., Pinkerton, H., 1996. Evolution of natrocarbonatite from a wollastonite nephelinite parent: evidence from the June, 1993 eruption of Oldoinyo Lengai, Tanzania. J. Geol. 104, 41–54.

Donaldson, C.H., Dawson, J.B., Kanaris-Sotiriou, R., Batchelor, R.A., Walsh, J.N., 1987. The silicate lavas of Oldoinyo Lengai, Tanzania. Neues Jahrb. Mineral. Abh. 156, 247–279.

Dunworth, E.A., Wilson, M., 1998. Olivine melilitites of the SW German Tertiary volcanic province: mineralogy and petrogenesis. J. Petrol. 39, 1805–1836.

Finkenbein, T., 2005. Petrologie und Vulkanologie der Riftflanke und des Sekenge-Kraters bei Engare Sero, East African Rift (Tanzania. Diploma thesis, University of Freiburg, 140 pp.

Furman, T., Bryce, J., Karson, J., Iotti, A., 2004. East African rift system (EARS) plume structure: insights from Quaternary mafic lavas of Turkana, Kenya. J. Petrol. 45, 1069–1088.

Hardarson, S.B., Fitton, G.J., 1991. Increased mantle melting beneath Snaefellsjökull volcano during Late Pleistocene deglaciation. Nature 353, 62–64.

Hay, R.L., 1983. Natrocarbonatite tephra of Kerimasi volcano, Tanzania. Geology 11, 599–602.

Hay, R.L., 1989. Holocene carbonatite–nephelinite tephra deposits of Oldoinyo Lengai, Tanzania. J. Volcanol. Geotherm. Res. 37, 77–91.

Hegner, E., Walter, H.J., Satir, M., 1995. Pb–Sr–Nd isotopic compositions and trace element geochemistry of megacrysts and melilitites from the Tertiary Urach volcanic field: source composition of small volume melts under SW Germany. Contrib. Mineral. Petrol. 122, 322–335.

Howie, R.A., Woolley, A.R., 1968. The role of titanium and the effect of TiO_2 on the cell-size, refractive index, and specific gravity in the andradite–melanite–schorlomite series. Mineral. Mag. 36, 775–790.

Johnson, L.H., Jones, A.P., Church, A.A., Taylor, W.R., 1997. Ultramafic xenoliths and megacrysts from a melilitite tuff cone, Deeti, northern Tanzania. J. Afr. Earth Sci. 25, 29–42.

Kalt, A., Hegner, E., Satir, M., 1997. Nd, Sr, and Pb isotopic evidence for lithospheric mantle sources of East African Rift carbonatites. Tectonophysics 278, 31–45.

Keller, J., 2002. Cone collapses, flank stability and hazard at Oldoinyo Lengai, Tanzania. IAVCEI International Congress, Montagne Pelée 1902-200. Abstracts, p. 68.

Keller, J., Krafft, M., 1990. Effusive natrocarbonatite activity of Oldoinyo Lengai, June 1988. Bull. Volcanol. 52, 629–645.

Keller, J., Spettel, B., 1995. The trace element composition and petrogenesis of natrocarbonatites. In: Bell, K., Keller, J. (Eds.), Carbonatite Volcanism: Oldoinyo Lengai and the Petrogenesis of Natrocarbonatites. IAVCEI Proceedings in Volcanology, vol. 4. Springer Verlag, Berlin, pp. 70–86.

Keller, J., Brey, G., Lorenz, V., Sachs, P., 1990. Volcanism and petrology of the Upper Rhinegraben (Urach-Hegau-Kaiserstuhl. IAVCEI International Volcanological Congress, Mainz 1990. Field Guide. 60 pp.

Klaudius, J., Keller, J., 2004. Quaternary debris avalanche deposits at Oldoinyo Lengai (Tanzania. IAVCEI General Assembly, Pucón, Chile 2004. Abstracts s02b_pth_048).

Klaudius, J., Keller, J., 2006-this issue. Peralkaline silicate lavas at Oldoinyo Lengai (Tanzania). Lithos 91, 173–190. doi:10.1016/j.lithos.2006.03.017.

Kjarsgaard, B.A., Hamilton, D.L., Peterson, T.D., 1995. Peralkaline nephelinite/carbonatite liquid immiscibility: comparison of phase composition in experiments and natural lavas from Oldoinyo Lengai. In: Bell, K., Keller, J. (Eds.), Carbonatite Volcanism: Oldoinyo Lengai and the Petrogenesis of Natrocarbonatites. IAVCEI Proceedings in Volcanology, vol. 4. Springer Verlag, Berlin, pp. 163–190.

Kramm, U., Sindern, S., 1998. Nd and Sr isotope signatures of fenites from Oldonio Lengai, Tanzania, and the genetic relationships between nephelinites, phonolites and carbonatites. J. Petrol. 39, 1997–2005.

Lee, W.J., Wyllie, P.J., 1994. Experimental data bearing on liquid immiscibility, crystal fractionation, and the origin of calcio-carbonatites and natrocarbonatites. Int. Geol. Rev. 36, 797–819.

Lee, W.J., Wyllie, P.J., 1998. Processes of crustal carbonatite formation by liquid immiscibility and differentiation, elucidated by model systems. J. Petrol. 39, 2005–2015.

Lee, C.T., Rudnick, R.L., McDonough, W.F., Horn, I., 2000. Petrologic and geochemical investigation of carbonates in peridotite xenoliths from northeastern Tanzania. Contrib. Mineral. Petrol. 139, 470–484.

Le Roex, A., Späth, A., Zartman, R., 2001. Lithospheric thickness beneath the southern Kenya Rift: implications from basalt geochemistry. Contrib. Mineral. Petrol. 142, 89–106.

Macdonald, R., Rogers, N.W., Fitton, J.G., Black, S., Smith, M., 2001. Plume–lithosphere interactions in the generation of the basalts of the Kenya Rift, East Africa. J. Petrol. 42, 877–900.

McDonough, W.F., Sun, S.S., 1995. The composition of the Earth. Chem. Geol. 120, 223–253.

McIntyre, R.M., Mitchell, J.G., Dawson, J.B., 1974. Age of the fault movements in the Tanzanian sector of the East African Rift system. Nature 247, 354–356.

Nyamweru, C., 1988. Activity of Oldoinyo Lengai Volcano, Tanzania, 1983–1987. J. Afr. Earth Sci. 7, 603–610.

Paslick, C., Halliday, A.M., James, D., Dawson, J.B., 1995. Enrichment of the continental lithosphere by OIB melts: isotopic evidence from the volcanic province of northern Tanzania. Earth Planet. Sci. Lett. 130, 109–126.

Peterson, T.D., 1989a. Peralkaline nephelinites. I. Comparative petrology of Shombole and Oldoinyo L'engai, East Africa. Contrib. Mineral. Petrol. 101, 458–478.

Peterson, T.D., 1989b. Peralkaline nephelinites: II. Low pressure fractionation and the hypersodic lavas of Oldoinyo Lengai. Contrib. Mineral. Petrol. 102, 336–346.

Peterson, T.D., 1990. Petrology and genesis of natrocarbonatite. Contrib. Mineral. Petrol. 105, 143–155.

Peterson, T.D., Kjarsgaard, B.A., 1995. What are the parental magmas at Oldoinyo Lengai? In: Bell, K., Keller, J. (Eds.), Carbonatite Volcanism: Oldoinyo Lengai and the Petrogenesis of Natrocarbonatites. IAVCEI Proceedings in Volcanology, vol. 4. Springer Verlag, Berlin, pp. 148–162.

Reck, H., 1914. Oldoinyo L'Engai, ein tätiger Vulkan im Gebiete der Deutsch-Ostafrikanischen Bruchstufe. Branca-Festschrift, Berlin, pp. 373–409.

SEAN, 1988. Oldoinyo Lengai, Tanzania. Small carbonatite lava lakes and flows. Smithson. Inst. Sci. Alert Netw. 13 (6), 2–3.

Simonetti, A., Bell, K., Shrady, C., 1997. Trace and rare-earth-element geochemistry of the June 1993 natrocarbonatite lavas, Oldoinyo Lengai (Tanzania): implications for the origin of carbonatite magmas. J. Volcanol. Geotherm. Res. 75, 89–106.

Sun, S.S., McDonough, W.F., 1989. Chemical and isotopic systematics of oceanic basalts: implications for mantle composition and processes. In: Saunders, A.D., Norry, M.J. (Eds.), Magmatism in the Oceanic Basins. . Geol. Soc. Special Publ., vol. 42. Blackwell Scientific Publications, Oxford, UK, pp. 313–345.

Uhlig, C., 1907. Der sogenannte Grosse Ostafrikanische Graben zwischen Magad (Natron See) und Lawa ya Mueri (Manyara See). Geogr. Z. 15, 478–505.

Velde, D., Yoder Jr., H.S., 1977. Melilite and melilite-bearing igneous rocks. Year B.-Carnegie Inst. Wash. 76, 478–485.

Wiedenmann, D., 2004. Vulkanologische Stellung und petrologische Interpretation der Biotit-Pyroxen-Olivin-Tuffe am Oldoinyo Lengai, Tansania. Diploma thesis, Freiburg, 89 pp.

Williams, R.W., Gill, J.B., Bruland, K.W., 1986. Ra–Th disequilibria systematics: timescale of carbonatite magma formation at Oldoinyo Lengai volcano, Tanzania. Geochim. Cosmochim. Acta 50, 1249–1259.

Wilson, M., Downes, H., 1991. Tertiary–Quaternary extension-related alkaline magmatism in western and central Europe. J. Petrol. 32, 811–849.

Wilson, M., Rosenbaum, J.M., Dunworth, E.A., 1995. Melilitites: partial melts of the thermal boundary layer? Contrib. Mineral. Petrol. 119, 181–196.